IEEE Access
Multidisciplinary : Rapid Review : Open Access Journal

Received 26 September 2023, accepted 7 November 2023, date of publication 13 November 2023,
date of current version 22 November 2023.

Digital Object Identifier 10.1109/ACCESS.2023.3332508

RESEARCH ARTICLE

Type Synthesis Method for Parallel Robots With Special Topologies

HONGPENG CHU[1,2], YIHUI ZHANG[3], YULIN ZHOU[3], AND DAXING ZENG[1]
[1]School of Mechanical Engineering, Dongguan University of Technology, Dongguan 523808, China
[2]School of Mechanical Engineering, Tianjin University, Tianjin 300072, China
[3]School of Mechanical Engineering, Yanshan University, Qinhuangdao 066004, China

Corresponding author: Daxing Zeng (zengdx@dgut.edu.cn)

This work was supported in part by the Guangdong Natural Science Foundation of China under Grant 2023A1515012103, in part by the Key Scientific Research Platforms and Projects of Guangdong Regular Institutions of Higher Education of China under Grant 2022KCXTD033, and in part by the Scientific Research Capacity Improvement Project of Key Developing Disciplines in Guangdong Province of China under Grant 2021ZDJS084.

ABSTRACT This contribution presents a type synthesis method for parallel robots with special topologies. First, we defined the constraint-incidence matrix (CIM) to describe serial chains by utilizing the geometric properties of screw theory, revealing the motion and constraint attributes and their internal relationship of serial chains. Then, a CIM-based synthesis method is proposed to convert the type synthesis of parallel robots into the geometric derivation of the CIM, and the specific operation steps of the proposed method are given. Finally, we demonstrated the application of the proposed method to the type synthesis of metamorphic, and wheeled parallel robots. Compared with existing type synthesis methods, the CIM-based synthesis method takes advantage of the known topological features of parallel robots with special topologies and can improve the efficiency of type synthesis.

INDEX TERMS Constraint-incidence matrix, geometric, parallel robot, screw theory, type synthesis.

I. INTRODUCTION

Parallel robots constitute an important branch of robotics with higher accuracy, bearing capacity, and dynamic performance than serial robots; accordingly, they are widely deployed in medical, aerospace, and mechanical automation applications [1]. The development of new parallel equipment is inseparable from that of innovative mechanisms, and parallel robot configurations can be systematically and comprehensively explored by type-synthesis theory assisted by mathematical tools.

Type-synthesis theory for parallel robots has developed rapidly over the past two decades, culminating in a variety of excellent type-synthesis methods [2], [3]. Type-synthesis methods are broadly divisible into motion- and constraint-based synthesis methods.

In motion-based synthesis methods, the motion of a parallel robot is determined by the intersection of the motions of all branches of the robot. Representative motion-based synthesis methods are based on Lie group theory. The representation of the spatial motions of rigid bodies by a displacement subgroup or Lie subgroup was pioneered by the French scholar Hervé [4], [5], [6], who deduced 12 kinds of displacement subgroups corresponding to 12 kinds of rigid body motions for the first time.

The Lie group theory-based synthesis method was later adopted by Lee and Hervé [7], [8], who synthesized a batch of mechanisms with Schoenflies motion, Li et al. [9], who synthesized a class of 3R2T parallel robots, where T denotes a translation DOF and R a rotational DOF, Angeles [10], who advanced the idea of a qualitative synthesis of parallel robots, and Li et al. [11], who studied the type synthesis of single-loop 3T1R parallel robots. Because not all rigid body motions satisfy the algebraic structure of Lie groups, Rico et al. [12], [13] analyzed the intersections of subgroups and subsets of the Euclidean group in detail, Meng et al. [14], [15] proposed a geometric synthesis theory, Li et al. [16], [17], [18], [19] developed a displacement manifold synthesis method. These approaches have extended the application scope of synthesis methods from those based on Lie group theory.

The associate editor coordinating the review of this manuscript and approving it for publication was Hui Xie.

Jin and Yang [20], [21], [22] proposed a POC-set synthesis method and synthesized a variety of 3-DOF parallel robots. Gogu [23], [24], [25] proposed a linear-transformation synthesis method based on the Jacobian matrix and comprehensively studied a class of fully isometric parallel robots. Gao and colleagues [26], [27], [28], [29] proposed a generalized function set (GF) synthesis method. Dai [30], Yang et al. [31], [32], and Sun et al. [33], [34], [35] proposed a finite-screw-type synthesis method based on the screw triangle product. Song et al. [36] synthesized a class of 2R1T parallel robots via conformal geometric algebra.

In constraint-based synthesis methods, the constraints of the moving platform of the mechanism are the union of all branch constraints. The representative method of constraint-based synthesis is the constraint-screw synthesis method proposed by Huang et al. [37], [38], which applies to any type of parallel robot and has led to the discovery of symmetrical 5-DOF parallel robots [39].

Based on constraint-screw theory, Fang and Tsai [40], [41], [42] carried out type syntheses on 3-, 4-, and 5-DOF parallel robots. Kong and Gosselin [43], [44], [45] conducted a type synthesis on a class of 3T, 3R1T, and spherical 3R parallel robots and later proposed a virtual-chain-type synthesis method [46], [47], Zeng and Huang [48] developed a number of parallel robots with rotational decoupling characteristics, and Xu et al. [49] synthesized 2R1T parallel robots with continuous rotation axes. Xie and Liu [50], [51], [52] proposed a visible synthesis method based on constraint-screw theory and Grassmann line geometry, which they applied to the type syntheses of 3-DOF and 4-DOF parallel robots suitable for manufacturing.

Based on the existing type synthesis methods, the DOF attribute of the desired parallel robot is used as a known condition, and branch structures and geometric relationships between the branches of the desired parallel robots are deduced inversely. In order to synthesize parallel robots with specific topologies using existing type synthesis methods, the topology of the parallel robots must be determined according to the DOF attributes of the parallel robots, and then the parallel robots with the desired topology are selected from the synthesis results.

Consider the possibility that some topological structures of parallel robots with special topologies can be determined. By using these topological structures as known conditions for type synthesis and directly synthesizing parallel robots with desired topologies and DOF attributes, the efficiency of type synthesis of parallel robots with special topologies will be significantly increased.

Based on the above motivation, a type synthesis method for parallel robots with special topologies is presented. First, the definition of the constraint-incidence matrix (CIM) is introduced. Then, the CIM-based synthesis method is proposed and the specific operation steps are given. Finally, we show the application of the proposed method to the type synthesis of metamorphic, and wheeled parallel robots.

II. CIM-BASED SYNTHESIS METHOD

A. CIM

A parallel robot is composed of a fixed platform and a moving platform connected by multiple serial chains that closely relate to the motion property of the robot. Therefore, the key to designing the desired parallel robot is to construct appropriate serial chains. A serial chain is generally composed of multiple kinematic pairs in series. In order to describe the geometric relationship between each kinematic pair in a serial chain, we defined the incidence matrix $\boldsymbol{Y}$ to describe a serial chain in Ref. [53]. According to constraint-screw theory [37], [39], it is not enough to only know the physical structure of a serial chain, but also need to know the constraint information. Therefore, we extend the definition of incidence matrix and propose the CIM $\boldsymbol{M}$ as shown in (1) to represent a serial chain [54].

$$\boldsymbol{M}=\begin{bmatrix}\boldsymbol{Y} & \boldsymbol{H}\\ \boldsymbol{L} & \boldsymbol{D}\end{bmatrix}=\left[\begin{array}{ccc|ccc}\boldsymbol{E}_1 & \cdots & \theta_{1i} & \theta_{1j} & \cdots & \theta_{1k}\\ \vdots & \ddots & \vdots & \vdots & \ddots & \vdots\\ g_{i1} & \cdots & \boldsymbol{E}_i & \theta_{ij} & \cdots & \theta_{ik}\\ \hline g_{j1} & \cdots & g_{ji} & \$_j & \cdots & \theta_{jk}\\ \vdots & \ddots & \vdots & \vdots & \ddots & \vdots\\ g_{k1} & \cdots & g_{ki} & g_{kj} & \cdots & \$_k\end{array}\right] \tag{1}$$

The CIM $\boldsymbol{M}$ is a block matrix consisting of subblocks $\boldsymbol{Y}$, $\boldsymbol{D}$, $\boldsymbol{L}$ and $\boldsymbol{H}$, each describing the different attributes of the serial chain. The incidence matrix $\boldsymbol{Y}$ describes the topological structure of the serial chain, and also corresponds to the motion-screw system of the serial chain. The main diagonal elements $\boldsymbol{E}_i$ of the incidence matrix $\boldsymbol{Y}$ represent the kinematic pairs in a serial chain, and the order of elements $\boldsymbol{E}_i$ corresponds to the connection order of the kinematic pairs in the serial chain. The lower and upper triangular matrices of the incidence matrix $\boldsymbol{Y}$ represent the positional and orientational relationships of kinematic pairs $\boldsymbol{E}_i$, respectively.

The subblock $\boldsymbol{D}$ represents the constraint-screw system of a serial chain, so it is also called the constraint matrix. The main diagonal elements $\$_j$ of the constraint matrix $\boldsymbol{D}$ correspond to the constraint screws of a serial chain. The lower and upper triangular matrices of the constraint matrix $\boldsymbol{D}$ represent the positional and orientational relationships of constraint screws $\$_j$, respectively. The subblocks $\boldsymbol{L}$ and $\boldsymbol{H}$ describe the positional and orientational relationships between the incidence matrix $\boldsymbol{Y}$ and the constraint matrix $\boldsymbol{D}$, respectively.

According to screw theory, the kinematic pairs represented by elements $\boldsymbol{E}_i$ can be divided into two types: the revolute pair $\boldsymbol{R}$ and the prismatic pair $\boldsymbol{P}$; the constraint screws represented by elements $\$_j$ can also be divided into two types: the constraint force $\boldsymbol{F}$ and the constraint couple $\boldsymbol{C}$.

The lower and upper triangular matrices of the CIM describe the positional and orientational relationships between the main diagonal elements, respectively. The geometric relationships corresponding to the values of the elements are shown in Table 1. In screw theory, prismatic pairs and constraint couples are expressed by free vectors, and

TABLE 1. Geometric relationships correspond to the values of the elements in the CIM.

Elements θ_{ij} in the upper triangular matrix	Orientational relationships	Elements g_{ji} in the lower triangular matrix	Positional relationships
π	Parallel	0	Non-intersect
$\pi/2$	Perpendicular	n	Intersect at point n (positive integer)
$u_{ij} \in \{(0,\pi/2)\cup(\pi/2,\pi)\}$	Neither parallel nor perpendicular	$0/n$	Non-intersect or intersect at point n
$v_{ij} \in \{(0,\pi/2)\cup(\pi/2,\pi]\}$	Non-perpendicular	$-n$	Intersection $-n$ is movable
$w_{ij} \in (0,\pi)$	Non-parallel	$\overline{n}$	Intersection $\overline{n}$ is instantaneous
$q_{ij} \in (0,\pi]$	Arbitrary	$\pm n$	Intersection $\pm n$ is fixed on one axis and movable on the other axis
$o_{ij} \in [-\pi,0)$	The angle varies with the motion of the serial chain		

a free vector has only direction and no position, therefore, the element g_{ji} related to prismatic pairs and constraint couples is always 0. Element $\theta_{ij} = o_{ij}$ indicates that the angle between two axes varies with the motion of the serial chain, and the angle o_{ij} is called the state angle. If a specific value $\varphi(\varphi > 0)$ is assigned to the state angle o_{ij}, the value of the state angle is instantaneous and recorded as $o_{ij} = -\varphi$.

A CIM $\boldsymbol{M}$ is essentially a matrix consisting of the motion-screw system and the constraint-screw system of a serial chain. In the CIM $\boldsymbol{M}$, the topology and constraint attributes of the serial chain are revealed, along with their internal relationships. Here is an example of how the CIM can be used to represent serial chains, as shown in the CIM $\boldsymbol{M}_1$ below.

$$\boldsymbol{M}_1 = \left[\begin{array}{ccccc:c} \boldsymbol{R}_1 & w_{12} & o_{13} & o_{13} & o_{13} & o_{13} \\ 1 & \boldsymbol{R}_2 & w_{23} & w_{23} & w_{23} & w_{23} \\ 0 & 2 & \boldsymbol{R}_3 & \pi & \pi & \pi \\ 0 & 0 & 0 & \boldsymbol{R}_4 & \pi & \pi \\ 0 & 0 & 0 & 0 & \boldsymbol{R}_5 & \pi \\ \cdots & \cdots & \cdots & \cdots & \cdots & \cdots \\ 1 & 1 & 0 & 0 & 0 & \boldsymbol{F}_6 \end{array}\right]$$

First, the topology of a serial chain can be determined by the subblock $\boldsymbol{Y}$ in the CIM $\boldsymbol{M}$. For example, according to the subblock $\boldsymbol{Y}$ in the CIM $\boldsymbol{M}_1$, the serial chain corresponding to $\boldsymbol{M}_1$ consists of five revolute pairs, in which the revolute pairs $\boldsymbol{R}_1$ and $\boldsymbol{R}_2$ intersect at point 1, the revolute pairs $\boldsymbol{R}_2$ and $\boldsymbol{R}_3$ intersect at point 2, and the revolute pairs $\boldsymbol{R}_3$, $\boldsymbol{R}_4$, and $\boldsymbol{R}_5$ are parallel to each other.

Second, the constraint-screw system of a serial chain can be determined according to the subblock $\boldsymbol{D}$ in the CIM $\boldsymbol{M}$. For example, according to the subblock $\boldsymbol{D}$ in the CIM $\boldsymbol{M}_1$, the constraint-screw system of the serial chain corresponding to $\boldsymbol{M}_1$ contains a constraint force $\boldsymbol{F}_6$.

Finally, according to the subblocks $\boldsymbol{L}$ and $\boldsymbol{H}$ in the CIM $\boldsymbol{M}$, the geometrical relationships between the constraint-screw system and the serial chain can also be obtained. For example, based on the subblocks $\boldsymbol{L}$ and $\boldsymbol{H}$ in the CIM $\boldsymbol{M}_1$, it can be known that the constraint force $\boldsymbol{F}_6$ crosses the intersection point 1 of the revolute pairs $\boldsymbol{R}_1$ and $\boldsymbol{R}_2$ and is parallel to the revolute pairs $\boldsymbol{R}_3$, $\boldsymbol{R}_4$, and $\boldsymbol{R}_5$.

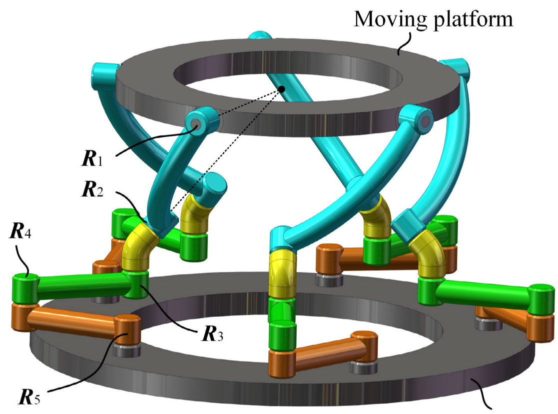

FIGURE 1. Symmetric 3R2T parallel robot.

We can efficiently design parallel robots using the CIM $\boldsymbol{M}$. For example, we want to design a symmetric 3R2T parallel robot based on the CIM $\boldsymbol{M}_1$. According to the DOF attribute of the desired parallel robot, the constraint forces supplied by the branches of the symmetric 3R2T parallel robot should be perpendicular to the fixed platform and coincide with each other. It is known that the serial chain corresponding to the CIM $\boldsymbol{M}_1$ can provide a constraint force $\boldsymbol{F}_6$, which crosses the intersection point 1 of the revolute pairs $\boldsymbol{R}_1$ and $\boldsymbol{R}_2$, and $\boldsymbol{F}_6$ is parallel to the revolute pairs $\boldsymbol{R}_3$, $\boldsymbol{R}_4$, and $\boldsymbol{R}_5$. Therefore, simply connect the revolute pair $\boldsymbol{R}_5$ vertically with the fixed platform to ensure that the constraint force $\boldsymbol{F}_6$ is perpendicular to the fixed platform; make the point 1 on the revolute pair $\boldsymbol{R}_1$ in each serial chain coincide to ensure that the constraint forces provided by all the serial chains coincide with each other. The final constructed symmetrical 3R2T parallel robot is shown in Fig. 1.

B. CIM-BASED SYNTHESIS METHOD

As shown in the above example, according to the CIM of a serial chain, not only the topology of the serial

TABLE 2. Mechanism-constraint systems for parallel robots.

DOF	MCM $\boldsymbol{D}_{\mathrm{M}}$	Mechanism-constraint system
3R2T	$\begin{bmatrix}\boldsymbol{F}_1\end{bmatrix}$	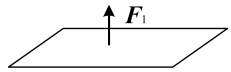
2R3T	$\begin{bmatrix}\boldsymbol{C}_1\end{bmatrix}$	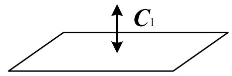
1R3T	$\begin{bmatrix}\boldsymbol{C}_1 & w_{12}\\ 0 & \boldsymbol{C}_2\end{bmatrix}$	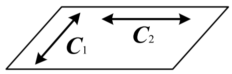
3R1T	$\begin{bmatrix}\boldsymbol{F}_1 & w_{12}\\ 1 & \boldsymbol{F}_2\end{bmatrix}$	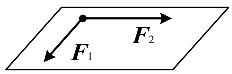
2R2T	$\begin{bmatrix}\boldsymbol{F}_1 & \pi\\ 0 & \boldsymbol{C}_2\end{bmatrix}\begin{bmatrix}\boldsymbol{F}_1 & \pi/2\\ 0 & \boldsymbol{C}_2\end{bmatrix}$	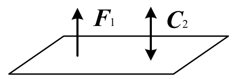 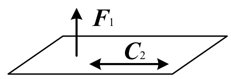
3R	$\begin{bmatrix}\boldsymbol{F}_1 & w_{12} & w_{13}\\ 1 & \boldsymbol{F}_2 & w_{23}\\ 1 & 1 & \boldsymbol{F}_3\end{bmatrix}$	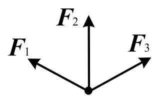
3T	$\begin{bmatrix}\boldsymbol{C}_1 & w_{12} & w_{13}\\ 0 & \boldsymbol{C}_2 & w_{23}\\ 0 & 0 & \boldsymbol{C}_3\end{bmatrix}$	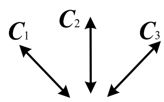
2R1T	$\begin{bmatrix}\boldsymbol{F}_1 & w_{12} & \pi/2\\ 1 & \boldsymbol{F}_2 & \pi/2\\ 0 & 0 & \boldsymbol{C}_3\end{bmatrix}\begin{bmatrix}\boldsymbol{F}_1 & w_{12} & w_{13}\\ 1 & \boldsymbol{F}_2 & w_{23}\\ 3 & 2 & \boldsymbol{F}_3\end{bmatrix}$	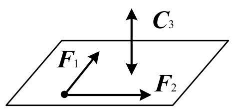 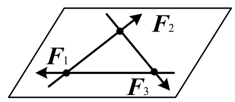
1R2T	$\begin{bmatrix}\boldsymbol{F}_1 & \pi/2 & \pi/2\\ 0 & \boldsymbol{C}_2 & w_{23}\\ 0 & 0 & \boldsymbol{C}_3\end{bmatrix}\begin{bmatrix}\boldsymbol{F}_1 & \pi & \pi\\ 0 & \boldsymbol{F}_2 & \pi\\ 0 & 0 & \boldsymbol{F}_3\end{bmatrix}$	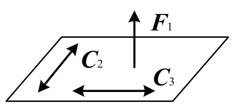 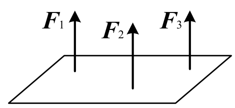

chain can be determined, but also the constraint-screw system of the serial chain can be obtained. More importantly, the CIM also reflects the geometrical relationship between the constraint-screw system and the serial chain. Therefore, if the CIMs of target serial chains can be derived from the DOF attributes and the structural design requirements of desired parallel robots, then the desired parallel robots can be conveniently designed. This method is called the CIM-based synthesis method and the specific synthesis process is summarised below:

Step 1: Determine the constraint matrix $\boldsymbol{D}$ of the target serial chain according to the DOF attribute requirements.

Step 2: Determine some elements in the incidence matrix $\boldsymbol{Y}$ of the target serial chain that meet the structural requirements.

Step 3: Determine the subblocks $\boldsymbol{L}$ and $\boldsymbol{H}$ in the CIM $\boldsymbol{M}$ based on the geometric constraints of reciprocal screws.

Step 4: Under the geometric constraints of the serial chain, deduce the remaining unknown elements in the CIM $\boldsymbol{M}$.

Step 5: According to the CIM $\boldsymbol{M}$, construct the desired parallel robot and verify its DOF attribute.

Below is a detailed description of each step.

Step 1: Determine the constraint matrix $\boldsymbol{D}$ *of the target serial chain*

For a parallel robot, its mechanism-constraint system represents the constraints of the moving platform, i.e., the DOFs that the moving platform do not possess. According to the definition of the constraint matrix [54], a constraint matrix can represent the spatial constraints of a rigid body. Therefore, the mechanism-constraint system and the limb-constraint system of a parallel robot can be expressed by the constraint matrices $\boldsymbol{D}_{\mathrm{M}}$ and $\boldsymbol{D}_{\mathrm{L}}$, respectively. The constraint matrices $\boldsymbol{D}_{\mathrm{M}}$ and $\boldsymbol{D}_{\mathrm{L}}$ are called mechanism-constraint matrix (MCM) and limb-constraint matrix (LCM), respectively.

Based on Table 9.3 in Ref. [55], this paper presents the mechanism-constraint systems for common types of parallel robots in the form of graphics and constraint matrices, as shown in Table 2. The constraint force and couple are represented by a single arrow line and a double arrow line, respectively. According to the DOF attribute requirements of the desired parallel robot, the mechanism-constraint system and the corresponding MCM $\boldsymbol{D}_{\mathrm{M}}$ of the desired parallel robot can be determined based on Table 2. The limb-constraint

TABLE 3. Structural classification of serial chains.

DOF	Excluding prismatic pairs	Including one prismatic pair	Including two prismatic pairs	Including three prismatic pairs
3-DOF	RRR.	PRR; RPR.	PPR; PRP.	PPP.
4-DOF	RRRR.	PRRR; RPRR.	PPRR; RPPR; PRPR; PRRP.	PPPR; PPRP.
5-DOF	RRRRR.	PRRRR; RPRRR; RRPRR.	PPRRR; RPPRR; PRPRR; RPRPR; PRRPR; PRRRP.	RRPPP; PRRPP; RPRPP; PRPRP; RPPRP; RPPPR.

system is a subset of the mechanism-constraint system, and the LCM $\boldsymbol{D}_{\mathrm{L}}$ is a submatrix of the MCM $\boldsymbol{D}_{\mathrm{M}}$. Therefore, the constraint matrix $\boldsymbol{D}$ of the target serial chain can be determined according to the MCM $\boldsymbol{D}_{\mathrm{M}}$ given in Table 2.

Step 2: Determine some elements in the incidence matrix $\boldsymbol{Y}$ *of the target serial chain*

The serial chains are classified by the type, number, and connection order of their kinematic pairs, and the structure of the serial chain is described by the main diagonal elements of the incidence matrix $\boldsymbol{Y}$. Table 3 shows all possible structures of 3-, 4-, and 5-DOF serial chains.

First, determine the values of some elements in the incidence matrix $\boldsymbol{Y}$ according to the structural design requirements, and then select one or more viable structures of the target serial chain from Table 3 to determine the main diagonal elements of the incidence matrix $\boldsymbol{Y}$.

Step 3: Determine the subblocks $\boldsymbol{L}$ *and* $\boldsymbol{H}$ *in the CIM* $\boldsymbol{M}$

For a serial chain, its kinematic pairs $\boldsymbol{E}_i$ and its constraint screws $\$_j$ are reciprocal screws to each other. Therefore, the position and orientation between the kinematic pairs and the constraint screws are mutually constrained, and the off-diagonal subblocks $\boldsymbol{L}$ and $\boldsymbol{H}$ describe the position and orientation constraints between $\boldsymbol{Y}$ and $\boldsymbol{D}$, respectively.

In screw theory, if any line vectors $\$_1 = [\boldsymbol{S}_1; \boldsymbol{r}_1 \times \boldsymbol{S}_1]$ and $\$_2 = [\boldsymbol{S}_2; \boldsymbol{r}_2 \times \boldsymbol{S}_2]$ are reciprocal screws to each other, then their reciprocal product is zero:

$$\begin{aligned} \$_1 \circ \$_2 &= \boldsymbol{S}_1 \cdot (\boldsymbol{r}_2 \times \boldsymbol{S}_2) + \boldsymbol{S}_2 \cdot (\boldsymbol{r}_1 \times \boldsymbol{S}_1) \\ &= (\boldsymbol{r}_2 - \boldsymbol{r}_1) \cdot (\boldsymbol{S}_1 \times \boldsymbol{S}_2) = 0 \end{aligned} \tag{2}$$

If (2) is true, then $\boldsymbol{r}_2 - \boldsymbol{r}_1 = \boldsymbol{0}$ or $\boldsymbol{S}_1 \times \boldsymbol{S}_2 = \boldsymbol{0}$. This result shows that line vectors are reciprocal screws to each other if and only if they intersect or are parallel to each other. If a line vector $\$_1 = [\boldsymbol{S}_1; \boldsymbol{r}_1 \times \boldsymbol{S}_1]$ and a free vector $\$_2 = [\boldsymbol{0}; \boldsymbol{S}_2]$ are reciprocal screws, then the following equation holds:

$$\$_1 \circ \$_2 = \boldsymbol{S}_1 \cdot \boldsymbol{S}_2 = 0. \tag{3}$$

According to (3), a line vector and a free vector are reciprocal screws if and only if they are perpendicular to each other. Clearly, two free vectors are always reciprocal screws to each other. The solution process of reciprocal screws mentioned above only applies to linear and free vectors without considering screws. If there are screw pairs in parallel robots, the CIM-based synthesis method is not applicable.

TABLE 4. Values of the elements in subblocks $\boldsymbol{L}$ and $\boldsymbol{H}$.

Constraint screw $\$_j$	Revolute pair $\boldsymbol{R}_i$	Prismatic pair $\boldsymbol{P}_i$
$\boldsymbol{F}_j$	$g_{ji} = n,\ \theta_{ij} = q_{ij}$; $g_{ji} = 0,\ \theta_{ij} = \pi$.	$g_{ji} = 0,\ \theta_{ij} = \pi / 2$.
$\boldsymbol{C}_j$	$g_{ji} = 0,\ \theta_{ij} = \pi / 2$.	$g_{ji} = 0,\ \theta_{ij} = q_{ij}$.

As a result of the above solution process of reciprocal screws, we can determine the values of the elements in subblocks $\boldsymbol{L}$ and $\boldsymbol{H}$. Table 4 specifies the elements in subblocks $\boldsymbol{L}$ and $\boldsymbol{H}$ for different elements $\$_j$ in the constraint matrix $\boldsymbol{D}$ and elements $\boldsymbol{E}_i$ in the incidence matrix $\boldsymbol{Y}$.

According to Table 4, the values of elements in subblocks $\boldsymbol{L}$ and $\boldsymbol{H}$ can be obtained based on the constraint screws $\$_j$ and the kinematic pairs $\boldsymbol{E}_i$ obtained in steps 1 and 2.

Step 4: Deduce the remaining unknown elements in the CIM $\boldsymbol{M}$

After implementing steps 1–3 of the type synthesis, the elements in the subblocks of $\boldsymbol{D}$, $\boldsymbol{L}$ and $\boldsymbol{H}$ and the main diagonal elements of the subblock $\boldsymbol{Y}$ are known, and the upper and lower triangular elements of the subblock $\boldsymbol{Y}$ remain to be determined. These unknown elements represent the geometric relationship between the kinematic pairs in the serial chain. Therefore, the essence of solving the CIM $\boldsymbol{M}$ is finding the possible geometric relationships between kinematic pairs $\boldsymbol{E}_i$ $(i = 1,2,3\cdots)$ under the geometric constraints of constraint screws $\$_j$ $(j = 1,2,3\cdots)$ on kinematic pairs $\boldsymbol{E}_i$.

For example, if a constraint force $\boldsymbol{F}$ is known to be parallel to revolute pairs $\boldsymbol{R}_1$, $\boldsymbol{R}_2$, and $\boldsymbol{R}_3$, then, according to the theorem of three parallel lines in space, the revolute pairs $\boldsymbol{R}_1$, $\boldsymbol{R}_2$, and $\boldsymbol{R}_3$ must be parallel to each other. To quickly obtain the desired CIM $\boldsymbol{M}$, the unknown elements in the CIM $\boldsymbol{M}$ can be solved by different methods based on geometric knowledge. The following are some tips or precautions for solving the CIM $\boldsymbol{M}$.

(a) Prioritize solving the positional and orientational relationships between adjacent kinematic pairs, and then judge the positional and orientational relationships between non-adjacent kinematic pairs.

(b) In general, there is no intersection between two non-adjacent revolute pairs; if there is a fixed intersection point n between non-adjacent revolute pairs $\boldsymbol{R}_i$ and $\boldsymbol{R}_j$, then only revolute pairs can exist between $\boldsymbol{R}_i$ and $\boldsymbol{R}_j$, and the revolute pair intersects with $\boldsymbol{R}_i$ and $\boldsymbol{R}_j$ at point n; if there is a non-fixed intersection point $-n$ or $\pm n$ between non-adjacent revolute pairs $\boldsymbol{R}_i$ and $\boldsymbol{R}_j$, the revolute pair and the prismatic pair between $\boldsymbol{R}_i$ and $\boldsymbol{R}_j$ must be perpendicular and parallel to the plane where $\boldsymbol{R}_i$ and $\boldsymbol{R}_j$ are located, respectively.

(c) When there are only prismatic pairs between non-adjacent kinematic pairs $\boldsymbol{E}_i$ and $\boldsymbol{E}_j$, the included angle θ_{ij} is a fixed angle; otherwise, $\theta_{ij} = o_{ij}$ is a variable angle.

(d) By the property of parallel lines, the angle between the kinematic pairs $\boldsymbol{E}_i$ and $\boldsymbol{E}_j$ and the angles between $\boldsymbol{E}_i$ and the kinematic pairs parallel to $\boldsymbol{E}_j$ should be equal.

(e) The axes of up to two revolute pairs can remain coplanar, and the coplanar axes of any three or more revolute pairs are instantaneous.

(f) For a serial chain without local DOF, up to three revolute pairs may intersect at one point and up to three adjacent revolute pairs may be parallel to each other.

Parallel robots with special topologies typically have design requirements for topological structures and connection relationships of branches, and some elements in the CIM $\boldsymbol{M}$ can be directly determined based on these design requirements. In addition, other unknown elements in the CIM $\boldsymbol{M}$ can be inferred from these elements which are directly determined by design requirements. Accordingly, the more structural design requirements for parallel robots, the more elements in the CIM $\boldsymbol{M}$ can be directly determined, and the easier it is to solve the CIM $\boldsymbol{M}$.

Step 5: Construct the desired parallel robot and verify its DOF attribute

To construct a parallel robot according to the synthesized serial chains, it is necessary to determine the geometric relationship between the serial chains. The geometrical relationships between the limb-constraint systems of the branches can be known from the mechanism-constraint system of the parallel robot, and the geometrical relationships between the limb-constraint system and the kinematic pairs in the serial chain can be known from the subblocks $\boldsymbol{L}$ and $\boldsymbol{H}$ of the CIM $\boldsymbol{M}$. Based on the above information, the geometric relationships between the serial chains that constitute the parallel robot can be deduced.

In the initial assembly position of the synthesized parallel robot, the DOF attributes generally meet design requirements. However, when the moving platform moves, the DOF attribute of the synthesized parallel robot cannot be guaranteed to meet design requirements. For this reason, the MCM $\boldsymbol{D}_{\mathrm{M}}$ of the synthesized parallel robot needs to be established to verify its DOF attribute. According to the definition of the constraint matrix, the mechanism-constraint system of a parallel robot can be expressed as:

$$\boldsymbol{D}_{\mathrm{M}} = \begin{bmatrix} \$_1 & \theta_{12} & \cdots & \theta_{1i} \\ g_{21} & \$_2 & \cdots & \theta_{2i} \\ \vdots & \vdots & \ddots & \vdots \\ g_{i1} & g_{i2} & \cdots & \$_i \end{bmatrix}.$$

The main diagonal elements $\$_i$ of the MCM $\boldsymbol{D}_{\mathrm{M}}$ represent the constraint screws exerted by each branch on the moving platform, and $\$_i$ can be determined according to the corresponding CIMs $\boldsymbol{M}$ of the branches. The upper and lower triangular matrices of the MCM $\boldsymbol{D}_{\mathrm{M}}$ represent the orientational and positional relationships between the constraint screws $\$_i$, respectively.

The geometric relationships between the constraint screws $\$_i$ and the moving or fixed platforms can be determined from the CIMs $\boldsymbol{M}$ of the branches. The moving and fixed platforms are two rigid bodies simultaneously connected to all branches. Therefore, the moving and fixed platforms can be used as objects of reference, the geometric relationships between the constraint screws $\$_i$ can be derived, and the values of each element in the upper and lower triangular matrices of the MCM $\boldsymbol{D}_{\mathrm{M}}$ can be determined.

In order to establish the MCM $\boldsymbol{D}_{\mathrm{M}}$ of the synthesized parallel robot, the moving and fixed platforms are used as reference objects. Therefore, it is necessary to consider the motion of the moving platform in relation to the fixed platform. However, we do not know the kinematics properties of the moving platform of the synthesized parallel robot, so we use the hypothetico-deductive method to verify the DOF attribute of the synthesized parallel robot, as follows:

(a) Assuming that the DOF attribute of the synthesized parallel robot is consistent with the mobility requirements in step 1, the geometric relationships between the moving and fixed platforms can be determined according to the DOF attribute of the desired parallel robot.

(b) The MCM $\boldsymbol{D}_{\mathrm{M}}$ of the synthesized parallel robot can be established based on the geometric relationships between the moving and fixed platforms.

(c) The MCMs of the desired and synthesized parallel robots are set as $\boldsymbol{D}_{\mathrm{M1}}$ and $\boldsymbol{D}_{\mathrm{M2}}$, respectively. If the MCMs $\boldsymbol{D}_{\mathrm{M1}}$ and $\boldsymbol{D}_{\mathrm{M2}}$ have the same order, and for any element $b_{ij} \in \boldsymbol{D}_{\mathrm{M2}}$, there is a corresponding element $a_{ij} \in \boldsymbol{D}_{\mathrm{M1}}$ that makes $|b_{ij}| \subseteq |a_{ij}|$ true. Then the hypothesis is valid, i.e., the DOF attribute of the synthesized parallel robot is consistent with the expected DOF attribute. Otherwise, the hypothesis is not valid, and the DOF attribute of the synthesized parallel robot does not meet the design requirements.

The following two considerations should be noted when verifying the DOF attribute of the synthesized parallel robot:

For over-constrained parallel robots, the constraint screws imposed by all branches on the moving platform are linearly correlated, i.e., the MCM $\boldsymbol{D}_{\mathrm{M2}}$ contains linearly correlated constraint screws. The constraint screws in the MCM $\boldsymbol{D}_{\mathrm{M2}}$ that are linearly correlated with the other constraint screws in $\boldsymbol{D}_{\mathrm{M2}}$ should be eliminated according to Table 2.1 in Ref. [55].

There is no specific requirement for the arrangement order of the main diagonal elements in the MCM $\boldsymbol{D}_{\mathrm{M}}$. To compare the relationship between the MCMs $\boldsymbol{D}_{\mathrm{M1}}$ and $\boldsymbol{D}_{\mathrm{M2}}$, the main diagonal elements of $\boldsymbol{D}_{\mathrm{M1}}$ and $\boldsymbol{D}_{\mathrm{M2}}$ should be arranged in the same order.

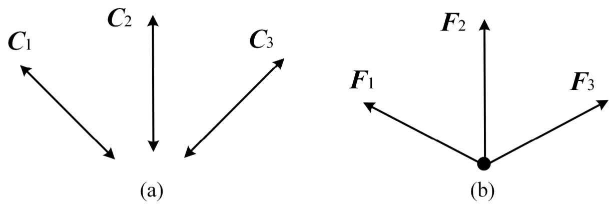

FIGURE 2. Mechanism-constraint systems for the 3T motion model (a) and the 3R motion model (b).

In the following sections, two kinds of parallel robots with special topologies are taken as examples to demonstrate the specific application of the CIM-based synthesis method.

III. TYPE SYNTHESES OF METAMORPHIC PARALLEL ROBOTS

Metamorphic parallel robots, also known as multi-mode parallel robots or reconfigurable parallel robots, can change their DOF attributes by changing their topology [56]. The commonly used ways to change the topology of metamorphic parallel robots can be summarized into two categories: changing the number of kinematic pairs in the mechanism, and changing the geometric relationship between certain kinematic pairs in the mechanism. Taking the 3T&3R metamorphic parallel robots as examples, the application of CIM-based synthesis method to metamorphic parallel robots will be demonstrated below.

A. DETERMINE THE CONSTRAINT MATRIX D OF THE TARGET SERIAL CHAIN

3R&3T metamorphic parallel robots have two kinds of DOF attributes, 3T and 3R. When the 3R&3T metamorphic parallel robots are in the 3T motion mode, the corresponding mechanism-constraint system is shown in Fig. 2(a).

The MCM of 3T parallel robots can be obtained as follows:

$$\boldsymbol{D}_{3\mathrm{T}} = \begin{bmatrix} \boldsymbol{C}_1 & w_{12} & w_{13} \\ 0 & \boldsymbol{C}_2 & w_{23} \\ 0 & 0 & \boldsymbol{C}_3 \end{bmatrix}. \tag{4}$$

The LCM is a submatrix of the MCM, so the constraint matrix of the target serial chains can contain 1, 2 or 3 constraint couples. Assuming that the target serial chains are 5-DOF chains, the corresponding constraint matrix of the target serial chains can be obtained as follows:

$$[\boldsymbol{C}]\,. \tag{5}$$

When the 3R&3T metamorphic parallel robots are in the 3R motion mode, the corresponding mechanism-constraint system and the MCM are shown in Fig. 2(b) and (6), respectively.

$$\boldsymbol{D}_{3\mathrm{R}} = \begin{bmatrix} \boldsymbol{F}_1 & w_{12} & w_{13} \\ 1 & \boldsymbol{F}_2 & w_{23} \\ 1 & 1 & \boldsymbol{F}_3 \end{bmatrix} \tag{6}$$

The LCM is a submatrix of the MCM, so the constraint matrix of the target serial chains can contain 1, 2 or 3 constraint forces. The target serial chains are 5-DOF chains, so the constraint matrix of the target serial chains contains a constraint force, as follows:

$$[\boldsymbol{F}]\,. \tag{7}$$

The target serial chains can provide two types of constraint-screw systems. Based on the definition of the CIM, we can further give the CIM corresponding to serial chains with two types of constraint-screw systems as:

$$\boldsymbol{M} = \begin{bmatrix} \boldsymbol{D}_1 & \boldsymbol{H}_1 & \boldsymbol{H}_{12} \\ \boldsymbol{L}_1 & \boldsymbol{Y} & \boldsymbol{H}_2 \\ \boldsymbol{L}_{12} & \boldsymbol{L}_2 & \boldsymbol{D}_2 \end{bmatrix}.$$

The constraint matrices $\boldsymbol{D}_1$ and $\boldsymbol{D}_2$ represent two types of constraint-screw systems. The subblocks $\boldsymbol{L}_1$ and $\boldsymbol{L}_2$ represent the positional relationships between the incidence matrix $\boldsymbol{Y}$ and the constraint matrices $\boldsymbol{D}_1$ and $\boldsymbol{D}_2$, respectively. The subblocks $\boldsymbol{H}_1$ and $\boldsymbol{H}_2$ show the orientational relationships between the incidence matrix $\boldsymbol{Y}$ and the constraint matrices $\boldsymbol{D}_1$ and $\boldsymbol{D}_2$, respectively. The subblocks $\boldsymbol{L}_{12}$ and $\boldsymbol{H}_{12}$ indicate the positional and orientational relationships between the constraint matrices $\boldsymbol{D}_1$ and $\boldsymbol{D}_2$, respectively.

B. DETERMINE SOME ELEMENTS IN THE INCIDENCE MATRIX Y OF THE TARGET SERIAL CHAIN

Taking the design method of changing the number of kinematic pairs in a serial chain as an example, the topology of the serial chain can be changed by locking different kinematic pairs in the serial chain. For example, a serial chain $R_1R_2R_3R_4R_5$ is composed of revolute pairs $\boldsymbol{R}_1$, $\boldsymbol{R}_2$, $\boldsymbol{R}_3$, $\boldsymbol{R}_4$, and $\boldsymbol{R}_5$ in series. The revolute pair $\boldsymbol{R}_1$ at the end of the serial chain can be locked to change the topology of the serial chain to $R_2R_3R_4R_5$, and the revolute pair $\boldsymbol{R}_2$ in the middle of the serial chain can also be locked to change the topology of the serial chain to $R_1R_3R_4R_5$.

However, locking the middle revolute pair $\boldsymbol{R}_2$ will change the geometric relationship between revolute pairs $\boldsymbol{R}_1$ and $\boldsymbol{R}_3$. Therefore, choosing a kinematic pair in the middle of a serial chain as a lockable kinematic pair not only changes the number of kinematic pairs, but also affects the geometric relationship between the related kinematic pairs, and metamorphic parallel robots composed of such reconfigurable chains can only switch its motion mode in a certain instantaneous position.

Choosing the kinematic pair at the end of the serial chain as the lockable kinematic pair only changes the number of kinematic pairs in the serial chain. Generally, a metamorphic parallel robot composed of such reconfigurable chains can change its motion mode at any time. Therefore, we choose the kinematic pairs at both ends of the target serial chains as lockable kinematic pairs. Based on (5) and (7), the CIM corresponding to the target serial chains can be obtained as follows:

$$
\boldsymbol{M}_3 = \left[\begin{array}{c:cccccc:c}
\boldsymbol{F}_0 & \theta_{01} & \theta_{02} & \theta_{03} & \theta_{04} & \theta_{05} & \backslash & \theta_{07} \\
\cdots & \cdots & \cdots & \cdots & \cdots & \cdots & \cdots & \cdots \\
g_{10} & \boldsymbol{E}_1 & \theta_{12} & \theta_{13} & \theta_{14} & \theta_{15} & \theta_{16} & \backslash \\
g_{20} & g_{21} & \boldsymbol{E}_2 & \theta_{23} & \theta_{24} & \theta_{25} & \theta_{26} & \theta_{27} \\
g_{30} & g_{31} & g_{32} & \boldsymbol{E}_3 & \theta_{34} & \theta_{35} & \theta_{36} & \theta_{37} \\
g_{40} & g_{41} & g_{42} & g_{43} & \boldsymbol{E}_4 & \theta_{45} & \theta_{46} & \theta_{47} \\
g_{50} & g_{51} & g_{52} & g_{53} & g_{54} & \boldsymbol{E}_5 & \theta_{56} & \theta_{57} \\
\backslash & g_{61} & g_{62} & g_{63} & g_{64} & g_{65} & \boldsymbol{E}_6 & \theta_{67} \\
\cdots & \cdots & \cdots & \cdots & \cdots & \cdots & \cdots & \cdots \\
g_{70} & \backslash & g_{72} & g_{73} & g_{74} & g_{75} & g_{76} & \boldsymbol{C}_7
\end{array}\right].
$$

where kinematic pairs $\boldsymbol{E}_1$ and $\boldsymbol{E}_6$ are lockable kinematic pairs, and element "\" indicates that the constraint screw is independent of the corresponding kinematic pair. For example, the constraint force $\boldsymbol{F}_0$ is independent of the kinematic pair $\boldsymbol{E}_6$, i.e., when the kinematic pair $\boldsymbol{E}_6$ is locked, the serial chain corresponding to the CIM $\boldsymbol{M}_3$ provides a constraint force $\boldsymbol{F}_0$.

Because prismatic pairs can make serial chains cumbersome, it is advisable to have at most one prismatic pair in the target serial chain, and this prismatic pair should be an active pair. The two motion modes of the 3R&3T metamorphic parallel robots are independent of each other, so there is no geometric constraint between the constraint screws $\boldsymbol{F}_0$ and $\boldsymbol{C}_7$ provided by the target serial chain. The CIMs corresponding to the target serial chain can be obtained as CIM $\boldsymbol{M}_{3.1}$, as shown in (8).

$$
\boldsymbol{M}_{3.1} = \left[\begin{array}{c:cccccc:c}
\boldsymbol{F}_0 & ? & ? & ? & ? & ? & \backslash & q_{07} \\
\cdots & \cdots & \cdots & \cdots & \cdots & \cdots & \cdots & \cdots \\
? & \boldsymbol{R}_1 & ? & ? & ? & ? & ? & \backslash \\
? & ? & \boldsymbol{R}_2 & ? & ? & ? & ? & ? \\
? & ? & ? & \boldsymbol{R}_3 & ? & ? & ? & ? \\
? & ? & ? & ? & \boldsymbol{R}_4 & ? & ? & ? \\
? & ? & ? & ? & ? & \boldsymbol{R}_5 & ? & ? \\
\backslash & ? & ? & ? & ? & ? & \boldsymbol{P}_6 & ? \\
\cdots & \cdots & \cdots & \cdots & \cdots & \cdots & \cdots & \cdots \\
0 & \backslash & ? & ? & ? & ? & ? & \boldsymbol{C}_7
\end{array}\right]. \quad (8)
$$

C. DETERMINE THE SUBBLOCKS L AND H IN THE CIM M

According to Table 4, values can be assigned to elements in the subblocks $\boldsymbol{L}$ and $\boldsymbol{H}$. According to the mechanism-constraint system shown in Fig. 2, the constraint force provided by each branch of the desired parallel robot is expected to intersect at one point, so the position of the constraint force $\boldsymbol{F}_0$ provided by the target serial chain is required to be determinable. When the prismatic pair $\boldsymbol{P}_6$ is locked, only the revolute pair $\boldsymbol{R}_1$ in the target serial chain is directly connected to the moving or fixed platforms. Therefore, it is necessary to intersect the constraint force $\boldsymbol{F}_0$ with the revolute pair $\boldsymbol{R}_1$ at a fixed point to determine the position of $\boldsymbol{F}_0$ relative to the fixed or moving platforms. The geometric relationship between the constraint force $\boldsymbol{F}_0$ and the revolute pair $\boldsymbol{R}_1$ can be determined as $\theta g_{ji} = n_{10},\ {}_{ij} = q_{01}$. As a result, the CIM $\boldsymbol{M}_{3.1}$ is as follows:

$$
\boldsymbol{M}_{3.1} = \left[\begin{array}{c:cccccc:c}
\boldsymbol{F}_0 & q_{01} & \pi(q_{02}) & \pi(q_{03}) & \pi(q_{04}) & \pi(q_{05}) & \backslash & q_{07} \\
\cdots & \cdots & \cdots & \cdots & \cdots & \cdots & \cdots & \cdots \\
n_{10} & \boldsymbol{R}_1 & ? & ? & ? & ? & ? & \backslash \\
0(n_{20}) & ? & \boldsymbol{R}_2 & ? & ? & ? & ? & \pi/2 \\
0(n_{30}) & ? & ? & \boldsymbol{R}_3 & ? & ? & ? & \pi/2 \\
0(n_{40}) & ? & ? & ? & \boldsymbol{R}_4 & ? & ? & \pi/2 \\
0(n_{50}) & ? & ? & ? & ? & \boldsymbol{R}_5 & ? & \pi/2 \\
\backslash & ? & ? & ? & ? & ? & \boldsymbol{P}_6 & q_{67} \\
\cdots & \cdots & \cdots & \cdots & \cdots & \cdots & \cdots & \cdots \\
0 & \backslash & 0 & 0 & 0 & 0 & 0 & \boldsymbol{C}_7
\end{array}\right].
$$

D. DEDUCE THE REMAINING UNKNOWN ELEMENTS IN THE CIM M

First, according to the geometric constraints imposed by the constraint couple $\boldsymbol{C}_7$ on the revolute pairs $\boldsymbol{R}_2$, $\boldsymbol{R}_3$, $\boldsymbol{R}_4$, $\boldsymbol{R}_5$, the geometric relationships between the revolute pairs $\boldsymbol{R}_2$, $\boldsymbol{R}_3$, $\boldsymbol{R}_4$, $\boldsymbol{R}_5$ can be deduced. When the four revolute pairs in the serial chain are all parallel to each other, they can be simultaneously perpendicular to the constraint couple $\boldsymbol{C}_7$. However, four parallel revolute pairs in a serial chain are linearly related, and at least two of the four revolute pairs in the serial chain are nonparallel. Two nonparallel revolute pairs uniquely determine the direction of the constraint couple $\boldsymbol{C}_7$, and the remaining revolute pairs must be parallel to one of the two revolute pairs. If the revolute pairs $\boldsymbol{R}_2$ and $\boldsymbol{R}_3$ are parallel to each other, then the revolute pairs $\boldsymbol{R}_3$, $\boldsymbol{R}_4$, and $\boldsymbol{R}_5$ must be parallel to each other, and some elements in the CIM $\boldsymbol{M}_{3.1}$ can be solved.

The constraint force $\boldsymbol{F}_0$ cannot intersect with three parallel revolute pairs $\boldsymbol{R}_3$, $\boldsymbol{R}_4$, and $\boldsymbol{R}_5$ simultaneously, so $\boldsymbol{F}_0$ can only be parallel with $\boldsymbol{R}_3$, $\boldsymbol{R}_4$, and $\boldsymbol{R}_5$. The revolute pairs $\boldsymbol{R}_2$ and $\boldsymbol{R}_3$ are not parallel, so the constraint force $\boldsymbol{F}_0$ can only intersect with $\boldsymbol{R}_2$.

It is known that the position of the constraint force $\boldsymbol{F}_0$ is determined by point n_{10} on the revolute pair $\boldsymbol{R}_1$, and $\boldsymbol{F}_0$ is parallel to revolute pairs $\boldsymbol{R}_3$, $\boldsymbol{R}_4$, and $\boldsymbol{R}_5$. Therefore, the position and direction of the constraint force $\boldsymbol{F}_0$ have been completely determined. The revolute pair $\boldsymbol{R}_2$ and the constraint force $\boldsymbol{F}_0$ are reciprocal screws to each other, so the intersection between $\boldsymbol{R}_2$ and $\boldsymbol{F}_0$ can only coincide with point n_{10}, i.e., the revolute pairs $\boldsymbol{R}_1$ and $\boldsymbol{R}_2$ intersect at point n_{10}. The solution of the CIM $\boldsymbol{M}_{3.1}$ is as follows:

$$\boldsymbol{M}_{3.1.1} = \begin{bmatrix} \boldsymbol{F}_0 & \vdots & o_{13} & w_{23} & \pi & \pi & \pi & \backslash & \vdots & q_{07} \\ \cdots & \vdots & \cdots & \cdots & \cdots & \cdots & \cdots & \cdots & \vdots & \cdots \\ 1 & \vdots & \boldsymbol{R}_1 & w_{12} & o_{13} & o_{13} & o_{13} & o_{16} & \vdots & \backslash \\ 1 & \vdots & 1 & \boldsymbol{R}_2 & w_{23} & w_{23} & w_{23} & o_{26} & \vdots & \pi/2 \\ 0 & \vdots & 0 & 0/2 & \boldsymbol{R}_3 & \pi & \pi & v_{56} & \vdots & \pi/2 \\ 0 & \vdots & 0 & 0 & 0 & \boldsymbol{R}_4 & \pi & v_{56} & \vdots & \pi/2 \\ 0 & \vdots & 0 & 0 & 0 & 0 & \boldsymbol{R}_5 & v_{56} & \vdots & \pi/2 \\ \backslash & \vdots & 0 & 0 & 0 & 0 & 0 & \boldsymbol{P}_6 & \vdots & q_{67} \\ \cdots & \vdots & \cdots & \cdots & \cdots & \cdots & \cdots & \cdots & \vdots & \cdots \\ 0 & \vdots & \backslash & 0 & 0 & 0 & 0 & 0 & \vdots & \boldsymbol{C}_7 \end{bmatrix} \tag{9}$$

Specifically, when the axes of the revolute pairs $\boldsymbol{R}_2$ and $\boldsymbol{R}_3$ intersect at one point, and this intersection coincides with the intersection of the revolute pairs $\boldsymbol{R}_1$ and $\boldsymbol{R}_2$, equation (9) evolves into:

$$\boldsymbol{M}_{3.1.2} = \begin{bmatrix} \boldsymbol{F}_0 & \vdots & o_{13} & w_{23} & \pi & \pi & \pi & \backslash & \vdots & q_{07} \\ \cdots & \vdots & \cdots & \cdots & \cdots & \cdots & \cdots & \cdots & \vdots & \cdots \\ 1 & \vdots & \boldsymbol{R}_1 & w_{12} & o_{13} & o_{13} & o_{13} & o_{16} & \vdots & \backslash \\ 1 & \vdots & 1 & \boldsymbol{R}_2 & w_{23} & w_{23} & w_{23} & o_{26} & \vdots & \pi/2 \\ 1 & \vdots & 1 & 1 & \boldsymbol{R}_3 & \pi & \pi & v_{56} & \vdots & \pi/2 \\ 0 & \vdots & 0 & 0 & 0 & \boldsymbol{R}_4 & \pi & v_{56} & \vdots & \pi/2 \\ 0 & \vdots & 0 & 0 & 0 & 0 & \boldsymbol{R}_5 & v_{56} & \vdots & \pi/2 \\ \backslash & \vdots & 0 & 0 & 0 & 0 & 0 & \boldsymbol{P}_6 & \vdots & q_{67} \\ \cdots & \vdots & \cdots & \cdots & \cdots & \cdots & \cdots & \cdots & \vdots & \cdots \\ 0 & \vdots & \backslash & 0 & 0 & 0 & 0 & 0 & \vdots & \boldsymbol{C}_7 \end{bmatrix} \tag{10}$$

E. CONSTRUCT THE DESIRED PARALLEL ROBOT AND VERIFY ITS DOF ATTRIBUTE

The CIMs $\boldsymbol{M}_{3.1.1}$ and $\boldsymbol{M}_{3.1.2}$ shown in (9) and (10) both meet our requirements. Taking the CIM $\boldsymbol{M}_{3.1.1}$ as an example, the desired 3T&3R metamorphic parallel robot can be designed.

The CIM $\boldsymbol{M}_{3.1.1}$ shows that the constraint couple $\boldsymbol{C}_7$ is perpendicular to the revolute pairs $\boldsymbol{R}_2$ and $\boldsymbol{R}_3$. According to the mechanism-constraint system for the 3T motion mode shown in Fig. 2, when multiple serial chains are connected to the moving and fixed platforms, it should be ensured that the vertical lines of the revolute pairs $\boldsymbol{R}_2$ and $\boldsymbol{R}_3$ in each serial chain are not parallel to each other.

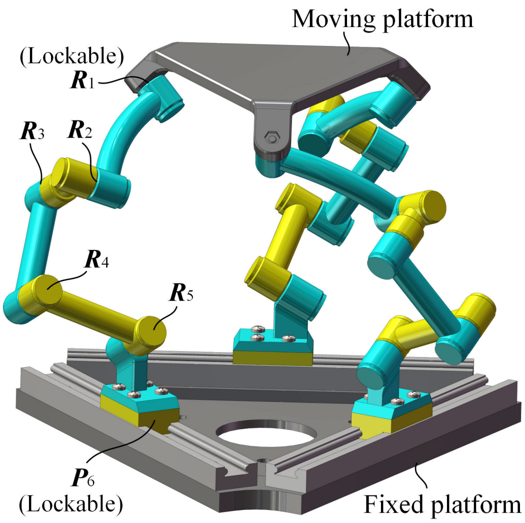

FIGURE 3. 3T&3R metamorphic parallel robot.

The CIM $\boldsymbol{M}_{3.1.1}$ shows that constraint force $\boldsymbol{F}_0$ passes through the intersection of the revolute pairs $\boldsymbol{R}_1$ and $\boldsymbol{R}_2$ and is parallel to the revolute pair $\boldsymbol{R}_5$. According to the mechanism-constraint system for the 3R motion mode shown in Fig. 2, when multiple serial chains are connected to the moving and fixed platforms, it should be ensured that the intersections of the revolute pairs $\boldsymbol{R}_1$ and $\boldsymbol{R}_2$ in each serial chain coincide with each other, and the revolute pairs $\boldsymbol{R}_5$ in each serial chain are neither parallel nor coplanar with each other. Finally, the desired 3T&3R metamorphic parallel robot can be designed, as shown in Fig. 3.

Next, verify whether the DOF attribute of the synthesized parallel robot meets the design requirements. If the DOF attribute of the synthesized parallel robot meets the design requirements, then the moving platform of the 3T&3R metamorphic parallel robot has six DOFs. As the moving platform can perform any motion relative to the fixed platform, there is no stable geometric relationship between the moving and fixed platforms.

When the revolute pair $\boldsymbol{R}_1$ in the CIM $\boldsymbol{M}_{3.1.1}$ is locked, the corresponding serial chain can exert a constraint couple $\boldsymbol{C}_7$ on the moving platform, and $\boldsymbol{C}_7$ is perpendicular to the revolute pairs $\boldsymbol{R}_2$ and $\boldsymbol{R}_3$. The directions of the revolute pairs $\boldsymbol{R}_2$ and $\boldsymbol{R}_3$ change with the movement of the serial chain, so the direction of the constraint couple $\boldsymbol{C}_7$ with respect to the moving or fixed platform cannot be determined. Under the 3T motion mode, the orientation between the constraint couples provided by the branches of the metamorphic parallel robot is variable, and the corresponding MCM can be obtained as follows:

$$\boldsymbol{D}_1 = \begin{bmatrix} \boldsymbol{C}_1 & o_{12} & o_{13} \\ 0 & \boldsymbol{C}_2 & o_{23} \\ 0 & 0 & \boldsymbol{C}_3 \end{bmatrix}. \tag{11}$$

When the prismatic pair $\boldsymbol{P}_6$ in the CIM $\boldsymbol{M}_{3.1.1}$ is locked, the corresponding serial chain can exert a constraint force $\boldsymbol{F}_0$ on the moving platform, and $\boldsymbol{F}_0$ passes through the intersection point 1 on the revolute pair $\boldsymbol{R}_1$ and is parallel to the revolute

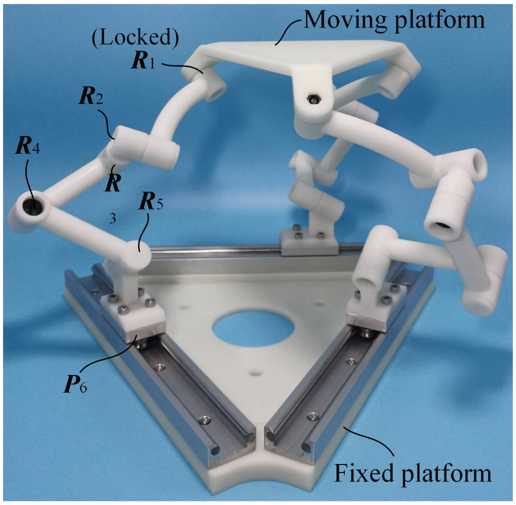

FIGURE 4. 3T&3R metamorphic parallel robot in 3T motion mode.

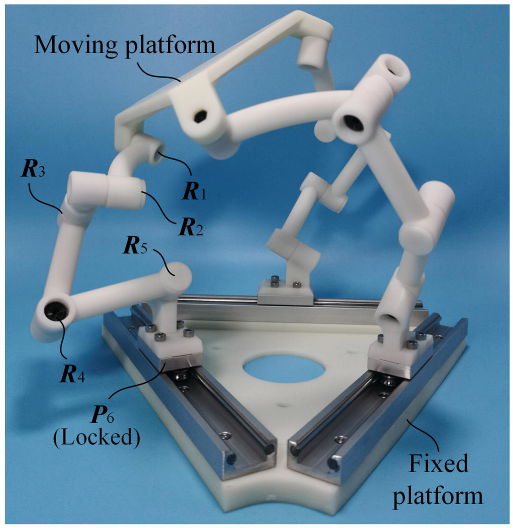

FIGURE 5. 3T&3R metamorphic parallel robot in 3R motion mode.

pair $\boldsymbol{R}_5$. The revolute pair $\boldsymbol{R}_1$ is connected to the moving platform, and point 1 is also a point on the moving platform, so the constraint force $\boldsymbol{F}_0$ passes through point 1 on the moving platform. There is a prismatic pair between the revolute pair $\boldsymbol{R}_5$ and the fixed platform, but the prismatic pair only changes the position but not the direction, so the direction of constraint force $\boldsymbol{F}_0$ relative to the fixed platform can still be determined, i.e., the constraint force $\boldsymbol{F}_0$ is neither parallel nor perpendicular to the fixed platform. Taking the moving and fixed platforms as reference objects, the MCM of the metamorphic parallel robot under the 3R motion mode can be obtained as:

$$\boldsymbol{D}_2 = \begin{bmatrix} \boldsymbol{F}_1 & w_{12} & w_{13} \\ 1 & \boldsymbol{F}_2 & w_{23} \\ 1 & 1 & \boldsymbol{F}_3 \end{bmatrix}. \tag{12}$$

By comparing (4) and (11), the orders of the MCMs $\boldsymbol{D}_1$ and $\boldsymbol{D}_{3\mathrm{T}}$ are equal, and for any element $b_{ij} \in \boldsymbol{D}_1$, there is a corresponding element $a_{ij} \in \boldsymbol{D}_{3\mathrm{T}}$, which makes $|b_{ij}| \subseteq |a_{ij}|$ true. As can be seen from (6) and (12), the CIMs $\boldsymbol{D}_2$ and $\boldsymbol{D}_{3\mathrm{R}}$ are identical. In summary, the assumption is valid, and the DOF attributes of the 3T&3R metamorphic parallel robot shown in Fig. 3 meet the design requirements.

It should be noted that we do not consider the case of elements $o_{ij} = \pi (ij = 12, 13, 23)$ in the MCM $\boldsymbol{D}_1$, because $o_{ij} = \pi$ indicates that the metamorphic parallel robot is in singular configuration, and the singularities of mechanisms are generally not considered during the type synthesis process.

The physical model of 3T&3R metamorphic parallel robot is made by 3D printing technology, as shown in Figs. 4 and 5. When the revolute pair $\boldsymbol{R}_1$ in each branch chain is locked, the moving platform of the 3T&3R metamorphic parallel robot has three translational DOFs and can move in any direction, as shown in Fig. 4.

When the prismatic pair $\boldsymbol{P}_6$ in each branch chain is locked, the moving platform of the 3T&3R metamorphic parallel robot has three rotational DOFs and can rotate along any axis, as shown in Fig. 5. Moreover, the 3T&3R metamorphic parallel robot can switch between 3T and 3R motion modes in any position and posture.

IV. TYPE SYNTHESES OF WHEELED PARALLEL ROBOTS

Wheels have the characteristics of unrestricted movement range. If wheels can be used in the design of parallel robots, then a class of wheeled parallel robots with large working space can be invented. The CIM-based synthesis method will be used to carry out the type synthesis of 6-DOF wheeled parallel robots.

A. DETERMINE THE CONSTRAINT MATRIX D OF THE TARGET SERIAL CHAIN

The branches of 6-DOF parallel robots are generally unconstrained chains, so the target serial chains should be 6-DOF serial chains with wheels. Because wheels can only move in one direction along their tangent, a steering DOF is usually required to allow the wheel to move in any direction. If a 6-DOF serial chain with wheels possesses steering DOF, it indicates that the serial chain has local DOF, i.e., only five of the six kinematic pairs of the serial chain are linearly independent. Therefore, the constraint-screw system of the target serial chain contains a constraint screw, which constrains the translational DOF perpendicular to the tangent direction of the wheel. The constraint matrix of the target serial chain can be obtained as follows:

$$\boldsymbol{D} = [\boldsymbol{F}].$$

B. DETERMINE SOME ELEMENTS IN THE INCIDENCE MATRIX Y OF THE TARGET SERIAL CHAIN

Set the rotational axis of the wheel as $\boldsymbol{R}_{\mathrm{w}}$, and the wheel can rotate around the vertical axis $\boldsymbol{R}_{\mathrm{t}}$, or move along the tangent line $\boldsymbol{P}_{\mathrm{w}}$ of the rim, as shown in Fig. 6. Therefore, the wheel has three motion axes, and the kinematic properties of the wheel can be represented by a 3×3 incidence matrix $\boldsymbol{W}_{\mathrm{G}}$,

TABLE 5. All possible CIMs corresponding to the target serial chains.

Type	CIM	Type	CIM
$\boldsymbol{M}_{4.1}$	$\begin{bmatrix} \boldsymbol{R}_{\mathrm{t}} & \pi/2 & \pi/2 & o_{14} & o_{15} & ? & \vdots & ? \\ 0 & \boldsymbol{P}_{\mathrm{w}} & \pi/2 & o_{24} & o_{25} & ? & \vdots & ? \\ 1 & 0 & \boldsymbol{R}_{\mathrm{w}} & w_{34} & o_{35} & ? & \vdots & ? \\ 1 & 0 & 1 & \boldsymbol{R}_4 & w_{45} & ? & \vdots & ? \\ 1 & 0 & 1 & 1 & \boldsymbol{R}_5 & ? & \vdots & ? \\ ? & ? & ? & ? & ? & \boldsymbol{R}_6 & \vdots & ? \\ \cdots & \cdots & \cdots & \cdots & \cdots & \cdots & \vdots & \cdots \\ ? & ? & ? & ? & ? & ? & \vdots & \boldsymbol{F}_7 \end{bmatrix}$	$\boldsymbol{M}_{4.2}$	$\begin{bmatrix} \boldsymbol{R}_{\mathrm{t}} & \pi/2 & \pi/2 & ? & o_{15} & o_{16} & \vdots & ? \\ 0 & \boldsymbol{P}_{\mathrm{w}} & \pi/2 & ? & o_{25} & o_{26} & \vdots & ? \\ 1 & 0 & \boldsymbol{R}_{\mathrm{w}} & ? & w_{35} & o_{36} & \vdots & ? \\ ? & ? & ? & \boldsymbol{P}_4 & ? & ? & \vdots & ? \\ 1 & 0 & 1 & ? & \boldsymbol{R}_5 & w_{56} & \vdots & ? \\ 1 & 0 & 1 & ? & 1 & \boldsymbol{R}_6 & \vdots & ? \\ \cdots & \cdots & \cdots & \cdots & \cdots & \cdots & \vdots & \cdots \\ ? & ? & ? & ? & ? & ? & \vdots & \boldsymbol{F}_7 \end{bmatrix}$
$\boldsymbol{M}_{4.3}$	$\begin{bmatrix} \boldsymbol{R}_{\mathrm{t}} & \pi/2 & \pi/2 & o_{14} & ? & o_{16} & \vdots & ? \\ 0 & \boldsymbol{P}_{\mathrm{w}} & \pi/2 & o_{24} & ? & o_{26} & \vdots & ? \\ 1 & 0 & \boldsymbol{R}_{\mathrm{w}} & w_{34} & ? & o_{36} & \vdots & ? \\ 1 & 0 & 1 & \boldsymbol{R}_4 & ? & w_{46} & \vdots & ? \\ ? & ? & ? & ? & \boldsymbol{P}_5 & ? & \vdots & ? \\ 1 & 0 & 1 & 1 & ? & \boldsymbol{R}_6 & \vdots & ? \\ \cdots & \cdots & \cdots & \cdots & \cdots & \cdots & \vdots & \cdots \\ ? & ? & ? & ? & ? & ? & \vdots & \boldsymbol{F}_7 \end{bmatrix}$	$\boldsymbol{M}_{4.4}$	$\begin{bmatrix} \boldsymbol{R}_{\mathrm{t}} & \pi/2 & \pi/2 & o_{14} & o_{15} & ? & \vdots & ? \\ 0 & \boldsymbol{P}_{\mathrm{w}} & \pi/2 & o_{24} & o_{25} & ? & \vdots & ? \\ 1 & 0 & \boldsymbol{R}_{\mathrm{w}} & w_{34} & o_{35} & ? & \vdots & ? \\ 1 & 0 & 1 & \boldsymbol{R}_4 & w_{45} & ? & \vdots & ? \\ 1 & 0 & 1 & 1 & \boldsymbol{R}_5 & ? & \vdots & ? \\ ? & ? & ? & ? & ? & \boldsymbol{P}_6 & \vdots & ? \\ \cdots & \cdots & \cdots & \cdots & \cdots & \cdots & \vdots & \cdots \\ ? & ? & ? & ? & ? & ? & \vdots & \boldsymbol{F}_7 \end{bmatrix}$

as follows:

$$\boldsymbol{W}_{\mathrm{G}} = \begin{bmatrix} \boldsymbol{R}_{\mathrm{t}} & \pi/2 & \pi/2 \\ 0 & \boldsymbol{P}_{\mathrm{w}} & \pi/2 \\ 1 & 0 & \boldsymbol{R}_{\mathrm{w}} \end{bmatrix}.$$

The wheel is regarded as a special multi-DOF kinematic pair and expressed by incidence matrix $\boldsymbol{W}_{\mathrm{G}}$, then the synthesis of the target serial chain is transformed into solving the CIM $\boldsymbol{M}$ containing the subblock $\boldsymbol{W}_{\mathrm{G}}$. The CIM $\boldsymbol{M}$ corresponding to the 6-DOF serial chains with wheels can be expressed as:

$$\boldsymbol{M}_4 = \begin{bmatrix} \boldsymbol{R}_{\mathrm{t}} & \boldsymbol{\pi}/2 & \boldsymbol{\pi}/2 & \theta_{14} & \theta_{15} & \theta_{16} & \vdots & \theta_{17} \\ 0 & \boldsymbol{P}_{\mathrm{w}} & \boldsymbol{\pi}/2 & \theta_{24} & \theta_{25} & \theta_{26} & \vdots & \theta_{27} \\ 1 & 0 & \boldsymbol{R}_{\mathrm{w}} & \theta_{34} & \theta_{35} & \theta_{36} & \vdots & \theta_{37} \\ g_{41} & g_{42} & g_{43} & \boldsymbol{E}_4 & \theta_{45} & \theta_{46} & \vdots & \theta_{47} \\ g_{51} & g_{52} & g_{53} & g_{54} & \boldsymbol{E}_5 & \theta_{56} & \vdots & \theta_{57} \\ g_{61} & g_{62} & g_{63} & g_{64} & g_{65} & \boldsymbol{E}_6 & \vdots & \theta_{67} \\ \cdots & \cdots & \cdots & \cdots & \cdots & \cdots & \vdots & \cdots \\ g_{71} & g_{72} & g_{73} & g_{74} & g_{75} & g_{76} & \vdots & \boldsymbol{F}_7 \end{bmatrix}.$$

According to screw theory, a serial chain can contain a maximum of three prismatic pairs. The serial chain with a wheel already contains a prismatic pair $\boldsymbol{P}_{\mathrm{w}}$, and the direction of $\boldsymbol{P}_{\mathrm{w}}$ can be changed through the steering DOF, which means that the serial chain already contains two prismatic pairs. Therefore, at most one of the unknown kinematic pairs $\boldsymbol{E}_4$, $\boldsymbol{E}_5$, and $\boldsymbol{E}_6$ can be prismatic pairs.

Wheels with steering freedom can move in any direction along the ground. Therefore, the revolute pair $\boldsymbol{R}_{\mathrm{t}}$ is linearly related to the other kinematic pairs in the serial chain. According to Grassmann line geometry [55], four lines intersecting at a point in space are linearly related, so four revolute pairs

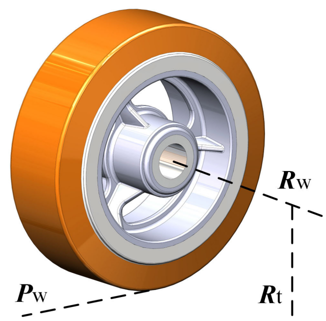

FIGURE 6. Wheel and its motion axes.

in the target serial chain can be made to intersect at the same point. All possible CIMs corresponding to the target serial chains with wheels are shown in Table 5.

C. DETERMINE THE SUBBLOCKS L AND H IN THE CIM M

The constraint force $\boldsymbol{F}_7$ should intersect or be parallel to revolute pairs and perpendicular to prismatic pairs. The elements in subblocks $\boldsymbol{L}$ and $\boldsymbol{H}$ of the CIMs shown in Table 5 can be solved, as shown in Table 6.

D. DEDUCE THE REMAINING UNKNOWN ELEMENTS IN THE CIM M

The CIM $\boldsymbol{M}_{4.1}$ indicates that revolute pairs $\boldsymbol{R}_{\mathrm{t}}$, $\boldsymbol{R}_{\mathrm{w}}$, $\boldsymbol{R}_4$, and $\boldsymbol{R}_5$ intersect at point 1, but the geometric relationships between revolute pair $\boldsymbol{R}_6$ and the other kinematic pairs remain unclear. The constraint force $\boldsymbol{F}_7$ passes through point 1 and is perpendicular to the prismatic pair $\boldsymbol{P}_{\mathrm{w}}$, therefore $\boldsymbol{F}_7$ is in the plane where the revolute pairs $\boldsymbol{R}_{\mathrm{t}}$ and $\boldsymbol{R}_{\mathrm{w}}$ are located. The point 2 should be the intersection of the revolute pair $\boldsymbol{R}_6$ and the plane where revolute pairs $\boldsymbol{R}_{\mathrm{t}}$ and $\boldsymbol{R}_{\mathrm{w}}$ are located. In general, the revolute pair $\boldsymbol{R}_6$ always intersects the plane where $\boldsymbol{R}_{\mathrm{t}}$ and $\boldsymbol{R}_{\mathrm{w}}$ are located, so $\boldsymbol{R}_6$ can have any geometric relationships with the other kinematic pairs in the serial chain, and the

TABLE 6. Solutions of the elements in subblocks L and H of the CIMs.

Type	CIM	Type	CIM
$\boldsymbol{M}_{4.1}$	$\left[\begin{array}{cccccc\|c} \boldsymbol{R}_t & \pi/2 & \pi/2 & o_{14} & o_{15} & ? & q_{17} \\ 0 & \boldsymbol{P}_w & \pi/2 & o_{24} & o_{25} & ? & \pi/2 \\ 1 & 0 & \boldsymbol{R}_w & w_{34} & o_{35} & ? & q_{37} \\ 1 & 0 & 1 & \boldsymbol{R}_4 & w_{45} & ? & q_{47} \\ 1 & 0 & 1 & 1 & \boldsymbol{R}_5 & ? & q_{57} \\ ? & ? & ? & ? & ? & \boldsymbol{R}_6 & q_{67} \\ \cdots & \cdots & \cdots & \cdots & \cdots & \cdots & \cdots \\ 1 & 0 & 1 & 1 & 1 & 2 & \boldsymbol{F}_7 \end{array}\right]$	$\boldsymbol{M}_{4.2}$	$\left[\begin{array}{cccccc\|c} \boldsymbol{R}_t & \pi/2 & \pi/2 & ? & o_{15} & o_{16} & q_{17} \\ 0 & \boldsymbol{P}_w & \pi/2 & ? & o_{25} & o_{26} & \pi/2 \\ 1 & 0 & \boldsymbol{R}_w & ? & w_{35} & o_{36} & q_{37} \\ ? & ? & ? & \boldsymbol{P}_4 & ? & ? & \pi/2 \\ 1 & 0 & 1 & ? & \boldsymbol{R}_5 & w_{56} & q_{57} \\ 1 & 0 & 1 & ? & 1 & \boldsymbol{R}_6 & q_{67} \\ \cdots & \cdots & \cdots & \cdots & \cdots & \cdots & \cdots \\ 1 & 0 & 1 & 0 & 1 & 1 & \boldsymbol{F}_7 \end{array}\right]$
$\boldsymbol{M}_{4.3}$	$\left[\begin{array}{cccccc\|c} \boldsymbol{R}_t & \pi/2 & \pi/2 & o_{14} & ? & o_{16} & q_{17} \\ 0 & \boldsymbol{P}_w & \pi/2 & o_{24} & ? & o_{26} & \pi/2 \\ 1 & 0 & \boldsymbol{R}_w & w_{34} & ? & o_{36} & q_{37} \\ 1 & 0 & 1 & \boldsymbol{R}_4 & ? & w_{46} & q_{47} \\ ? & ? & ? & ? & \boldsymbol{P}_5 & ? & \pi/2 \\ 1 & 0 & 1 & 1 & ? & \boldsymbol{R}_6 & q_{67} \\ \cdots & \cdots & \cdots & \cdots & \cdots & \cdots & \cdots \\ 1 & 0 & 1 & 1 & 0 & 1 & \boldsymbol{F}_7 \end{array}\right]$	$\boldsymbol{M}_{4.4}$	$\left[\begin{array}{cccccc\|c} \boldsymbol{R}_t & \pi/2 & \pi/2 & o_{14} & o_{15} & ? & q_{17} \\ 0 & \boldsymbol{P}_w & \pi/2 & o_{24} & o_{25} & ? & \pi/2 \\ 1 & 0 & \boldsymbol{R}_w & w_{34} & o_{35} & ? & q_{37} \\ 1 & 0 & 1 & \boldsymbol{R}_4 & w_{45} & ? & q_{47} \\ 1 & 0 & 1 & 1 & \boldsymbol{R}_5 & ? & q_{57} \\ ? & ? & ? & ? & ? & \boldsymbol{P}_6 & \pi/2 \\ \cdots & \cdots & \cdots & \cdots & \cdots & \cdots & \cdots \\ 1 & 0 & 1 & 1 & 1 & 0 & \boldsymbol{F}_7 \end{array}\right]$

solution of the CIM $\boldsymbol{M}_{4.1}$ can be obtained as follows:

$$\boldsymbol{M}_{4.1} = \left[\begin{array}{cccccc|c} \boldsymbol{R}_t & \pi/2 & \pi/2 & o_{14} & o_{15} & o_{16} & q_{17} \\ 0 & \boldsymbol{P}_w & \pi/2 & o_{24} & o_{25} & o_{26} & \pi/2 \\ 1 & 0 & \boldsymbol{R}_w & w_{34} & o_{35} & o_{36} & q_{37} \\ 1 & 0 & 1 & \boldsymbol{R}_4 & w_{45} & o_{46} & q_{47} \\ 1 & 0 & 1 & 1 & \boldsymbol{R}_5 & q_{56} & q_{57} \\ 0 & 0 & 0 & 0 & 0/3 & \boldsymbol{R}_6 & q_{67} \\ \cdots & \cdots & \cdots & \cdots & \cdots & \cdots & \cdots \\ 1 & 0 & 1 & 1 & 1 & 2 & \boldsymbol{F}_7 \end{array}\right].$$

It should be noted that when the revolute pairs $\boldsymbol{R}_5$ and $\boldsymbol{R}_6$ intersect at point 3, the element $q_{56} \neq \pi$, otherwise $\boldsymbol{R}_5$ and $\boldsymbol{R}_6$ coincide with each other, i.e., $\boldsymbol{R}_5$ and $\boldsymbol{R}_6$ are linearly correlated.

The CIM $\boldsymbol{M}_{4.2}$ indicates that the revolute pairs $\boldsymbol{R}_t$, $\boldsymbol{R}_w$, $\boldsymbol{R}_5$, and $\boldsymbol{R}_6$ intersect at point 1, but the geometric relationships between the prismatic pair $\boldsymbol{P}_4$ and the other kinematic pairs remain unclear. The prismatic pair $\boldsymbol{P}_4$ is located between the revolute pairs $\boldsymbol{R}_w$ and $\boldsymbol{R}_5$, and the motion of the prismatic pair $\boldsymbol{P}_4$ will inevitably lead to points on $\boldsymbol{R}_w$ not coincident with points on $\boldsymbol{R}_5$. Therefore, the CIM $\boldsymbol{M}_{4.2}$ has no solution.

According to the CIM $\boldsymbol{M}_{4.3}$, the revolute pairs $\boldsymbol{R}_t$, $\boldsymbol{R}_w$, $\boldsymbol{R}_4$, and $\boldsymbol{R}_6$ intersect at point 1, and the geometric relationships between the prismatic pair $\boldsymbol{P}_5$ and the other kinematic pairs need to be determined. The motion of the prismatic pair $\boldsymbol{P}_5$ cannot affect the revolute pair $\boldsymbol{R}_6$ passing through point 1, so $\boldsymbol{P}_5$ can only be parallel to $\boldsymbol{R}_6$, and the intersection point 1 is a movable point on $\boldsymbol{R}_6$. The CIM $\boldsymbol{M}_{4.3}$ can be solved as follows:

$$\boldsymbol{M}_{4.3} = \left[\begin{array}{cccccc|c} \boldsymbol{R}_t & \pi/2 & \pi/2 & o_{14} & o_{15} & o_{15} & q_{17} \\ 0 & \boldsymbol{P}_w & \pi/2 & o_{24} & o_{25} & o_{25} & \pi/2 \\ 1 & 0 & \boldsymbol{R}_w & w_{34} & o_{35} & o_{35} & q_{37} \\ 1 & 0 & 1 & \boldsymbol{R}_4 & w_{45} & w_{45} & q_{47} \\ 0 & 0 & 0 & 0 & \boldsymbol{P}_5 & \pi & \pi/2 \\ \pm 1 & 0 & \pm 1 & \pm 1 & 0 & \boldsymbol{R}_6 & \pi/2 \\ \cdots & \cdots & \cdots & \cdots & \cdots & \cdots & \cdots \\ 1 & 0 & 1 & 1 & 0 & 1 & \boldsymbol{F}_7 \end{array}\right].$$

According to the CIM $\boldsymbol{M}_{4.4}$, the revolute pairs $\boldsymbol{R}_t$, $\boldsymbol{R}_w$, $\boldsymbol{R}_4$, and $\boldsymbol{R}_5$ intersect at point 1, and the geometric relationships between the prismatic pair $\boldsymbol{P}_6$ and the other kinematic pairs remain unclear. The geometric relationship between the prismatic pair $\boldsymbol{P}_6$ and the revolute pair $\boldsymbol{R}_5$ does not affect the geometric relationship between $\boldsymbol{R}_5$ and the other kinematic pairs. Therefore, there can be any geometric relationship between the prismatic pair $\boldsymbol{P}_6$ and the revolute pair $\boldsymbol{R}_5$, and the CIM $\boldsymbol{M}_{4.4}$ can be solved as follows:

$$\boldsymbol{M}_{4.4} = \left[\begin{array}{cccccc|c} \boldsymbol{R}_t & \pi/2 & \pi/2 & o_{14} & o_{15} & o_{16} & q_{17} \\ 0 & \boldsymbol{P}_w & \pi/2 & o_{24} & o_{25} & o_{26} & \pi/2 \\ 1 & 0 & \boldsymbol{R}_w & w_{34} & o_{35} & o_{36} & q_{37} \\ 1 & 0 & 1 & \boldsymbol{R}_4 & w_{45} & o_{46} & q_{47} \\ 1 & 0 & 1 & 1 & \boldsymbol{R}_5 & q_{56} & q_{57} \\ 0 & 0 & 0 & 0 & 0 & \boldsymbol{P}_6 & \pi/2 \\ \cdots & \cdots & \cdots & \cdots & \cdots & \cdots & \cdots \\ 1 & 0 & 1 & 1 & 1 & 0 & \boldsymbol{F}_7 \end{array}\right].$$

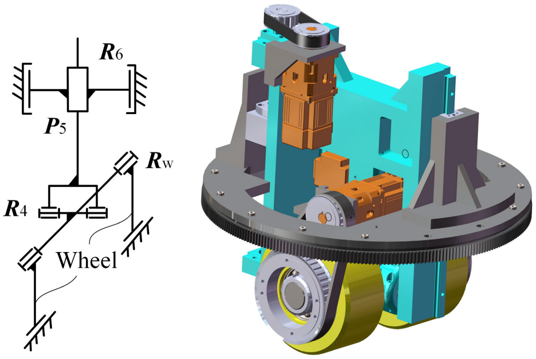

FIGURE 7. Serial chain corresponding to the CIM $M_{4.3}$.

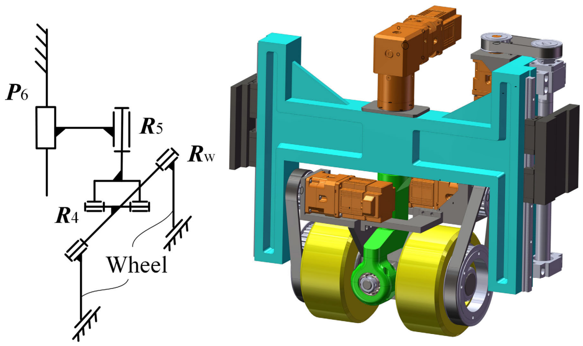

FIGURE 8. Serial chain corresponding to the CIM $M_{4.4}$.

E. CONSTRUCT THE DESIRED PARALLEL ROBOT AND VERIFY ITS DOF ATTRIBUTE

Wheeled parallel robots are reconfigurable mechanisms, and their DOF attributes change with the combination state of the wheels. Therefore, in this step, we need to verify the mobility of the wheeled parallel robot before constructing it. Mobile robots generally have four wheels, so we take a wheeled parallel robot composed of four serial chains with wheels as an example to analyze the mobility of the wheeled parallel robot.

The first type of wheeled parallel robots is composed of serial chains corresponding to the CIM $M_{4.1}$, and the constraint force provided by the serial chain passes through points 1 and 2 in the serial chain and is perpendicular to the translational axis P_w. Assume that the revolute pair R_6 in each serial chain is vertically connected with the moving platform, and the constraints exerted by the four serial chains on the moving platform are F_1, F_2, F_3, and F_4, respectively. Establish a reference coordinate system O-*XYZ* on the moving platform; P_X, P_Y, and P_Z denote the translational DOFs along the X, Y, and Z axes, respectively; R_X, R_Y, and R_Z denote the rotational DOFs around the X, Y, and Z axes, respectively. The DOF attributes of the first type of wheeled parallel robots are shown in Table 7.

The direction of translational DOF should be perpendicular to all constraint forces, and the axis of rotational DOF should intersect or be parallel to all constraint forces. Therefore, the DOF attributes of the first type of wheeled parallel robots corresponding to topological structures 1, 2, and 3 are P_X, P_Y, and R_Z, respectively. The first type of wheeled parallel robot does not have the expected mobility, so the CIM $M_{4.1}$ is abandoned.

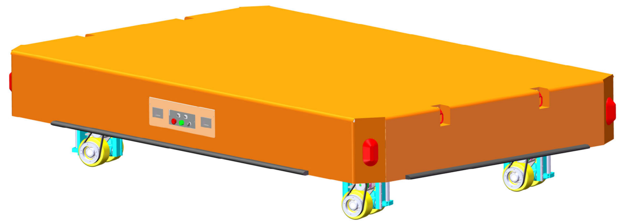

FIGURE 9. 6-DOF wheeled parallel robot.

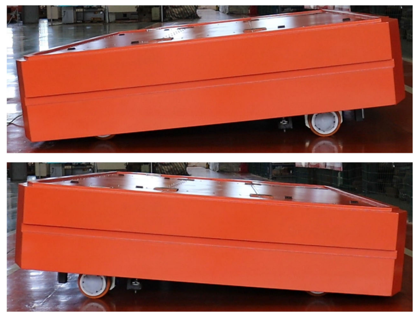

FIGURE 10. Demonstration of the rotational DOF around the X-axis.

FIGURE 11. Demonstration of the rotational DOF around the Y-axis.

The second type of wheeled parallel robots is composed of serial chains corresponding to the CIM $M_{4.3}$, and the constraint force provided by the serial chain passes through point 1 in the serial chain and is perpendicular to the translational axis P_w and the revolute pair R_6. Assume that the revolute pair R_6 in each serial chain is vertically connected with the moving platform, and the DOF attributes of the second type of wheeled parallel robots are shown in Table 8. The second type of wheeled parallel robots can achieve all six DOFs through a variety of wheel combinations, which satisfies the mobility requirements.

The third type of wheeled parallel robots is composed of serial chains corresponding to the CIM $M_{4.4}$, and the constraint force provided by the serial chain passes through point 1 in the serial chain and is perpendicular to the translational axis P_w and the prismatic pair P_6. Assume that the prismatic pair P_6 in each serial chain is vertically connected with the moving platform, then the DOF attributes of the third type of wheeled parallel robots are identical to the DOF attributes of the second type of wheeled parallel robots. Table 8 shows

TABLE 7. DOF attributes of the first type of wheeled parallel robots.

Types	Wheels	Mechanism-constraint systems	Relationships	DOFs
Topological structure1	Axes $\boldsymbol{R}_w$ of wheels are perpendicular to the X-axis.	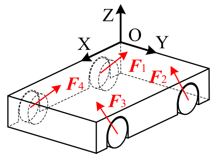	$\boldsymbol{F}_1$, $\boldsymbol{F}_2$, $\boldsymbol{F}_3$, and $\boldsymbol{F}_4$ are perpendicular to the X-axis.	$\boldsymbol{P}_X$
Topological structure 2	Axes $\boldsymbol{R}_w$ of wheels are perpendicular to the Y-axis.	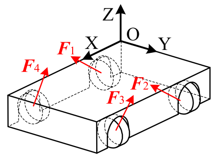	$\boldsymbol{F}_1$, $\boldsymbol{F}_2$, $\boldsymbol{F}_3$, and $\boldsymbol{F}_4$ are perpendicular to the Y-axis.	$\boldsymbol{P}_Y$
Topological structure 3	Axes $\boldsymbol{R}_w$ of two diagonal wheels are coplanar.	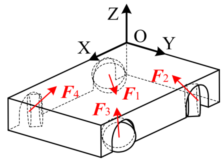	$\boldsymbol{F}_1$ and $\boldsymbol{F}_3$ are coplanar; $\boldsymbol{F}_2$ and $\boldsymbol{F}_4$ are coplanar.	$\boldsymbol{R}_Z$

TABLE 8. DOF attributes of the second type of wheeled parallel robots.

Types	Wheels	Mechanism-constraint systems	Relationships	DOFs
Topological structure1	Axes $\boldsymbol{R}_w$ of wheels are perpendicular to the X-axis.	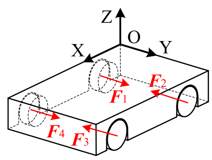	$\boldsymbol{F}_1$, $\boldsymbol{F}_2$, $\boldsymbol{F}_3$, and $\boldsymbol{F}_4$ are perpendicular to the XOZ-plane.	$\boldsymbol{P}_X$, $\boldsymbol{P}_Z$, $\boldsymbol{R}_Y$
Topological structure 2	Axes $\boldsymbol{R}_w$ of wheels are perpendicular to the Y-axis.	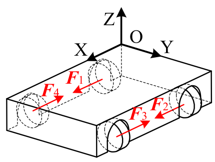	$\boldsymbol{F}_1$, $\boldsymbol{F}_2$, $\boldsymbol{F}_3$, and $\boldsymbol{F}_4$ are perpendicular to the YOZ-plane.	$\boldsymbol{P}_Y$, $\boldsymbol{P}_Z$, $\boldsymbol{R}_X$
Topological structure 3	Axes $\boldsymbol{R}_w$ of two diagonal wheels are coplanar.	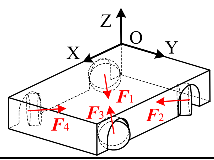	$\boldsymbol{F}_1$, $\boldsymbol{F}_2$, $\boldsymbol{F}_3$, and $\boldsymbol{F}_4$ are perpendicular to the Z-axis; $\boldsymbol{F}_1$ and $\boldsymbol{F}_3$ are coplanar; $\boldsymbol{F}_2$ and $\boldsymbol{F}_4$ are coplanar.	$\boldsymbol{P}_Z$, $\boldsymbol{R}_Z$

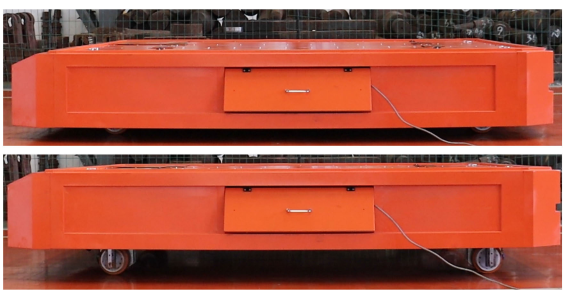

FIGURE 12. Demonstration of the translational DOF along the Z-axis.

that the third type of wheeled parallel robots can achieve all six DOFs by changing the wheel combination states, which meets the mobility requirements.

According to the CIM $\boldsymbol{M}_{4.3}$ and $\boldsymbol{M}_{4.4}$, the corresponding serial chains with wheels can be designed, as shown in Figs. 7 and 8 [57]. The desired 6-DOF wheeled parallel robots can be designed by connecting four serial chains as shown in Figs. 7 or 8 with the moving platform. Fig. 9 shows a 6-DOF wheeled parallel robot consisting of four serial chains corresponding to the CIM $\boldsymbol{M}_{4.4}$.

The 6-DOF wheeled parallel robot possesses the kinematic properties of both mobile robots and parallel robots. It can not only move in a large range like mobile robots, but also can adjust the posture and height of the moving platform like parallel robots. as shown in Figs. 10-12.

V. CONCLUSION

The CIM comprehensively reveals the motion and constraint attributes and their internal relationship within the serial chain. Based on the CIM, this paper presents a CIM-based synthesis method for parallel robots with special topologies.

The CIM-based synthesis method is based on the geometric properties of screw theory, and converts the type synthesis of parallel robots into the solutions of the CIM. Additionally, the proposed method employs geometric derivations to solve the CIM, avoids complicated algebraic and set operations, and has the advantages of intuitive and easy operation.

In comparison to existing type synthesis methods, the CIM-based synthesis method takes advantage of the known topological features of parallel robots with special topologies. Based on these known topological features, the values of relevant elements in the CIM corresponding to the target serial chains can be directly determined. The more constraints on the structural design of parallel robots, the more recognizable elements in the CIM, and the easier it is to solve the CIM. Comparing Section IV and [57], it can be seen that it took several weeks to synthesize and select the configurations of wheeled parallel robots before, but now it only takes a few hours to obtain the same synthesis result using the CIM-based synthesis method. Therefore, the CIM-based synthesis method is suitable for parallel robots with special topologies and can improve the efficiency of type synthesis.

For the type synthesis of ordinary parallel robot, the known information is only the DOF attribute of the desired parallel robot. If the target serial chains are synthesized according to steps 1-4 in Section II, the corresponding CIMs generally have multiple solutions, and solving CIMs will take a lot of work. For this reason, the authors have carried out a systematic derivation of the commonly used 3-,4-,5-DOF serial chains and compiled them into a serial-chain database [54]. The serial-chain database lists 97 kinds of commonly used serial chains, and divides these 97 kinds of serial chains into ten categories according to the constraint-screw system of serial chains. Readers can search the target serial chains in the database according to the constraint-screw system of the desired parallel robot, then steps 1-4 of the CIM-based synthesis method can be omitted, and the desired parallel robot can be designed directly according to the searched serial chains. Therefore, the CIM-based synthesis method is also suitable for the design of ordinary parallel robots, and the type-synthesis efficiency of ordinary parallel robots can be improved with the aid of the serial-chain database.

ACKNOWLEDGMENT

The author Hongpeng Chu would like to thank to Prof. Zhen Huang of Yanshan University for his critical discussion and reading during manuscript preparation.

REFERENCES

[1] Z. Pandilov and V. Dukovski, "Comparison of the characteristics between serial and parallel robots," *Acta Techn. Corvininesis-Bull. Eng.*, vol. 7, no. 1, pp. 143–160, 2014.

[2] X. Meng, F. Gao, S. Wu, and Q. J. Ge, "Type synthesis of parallel robotic mechanisms: Framework and brief review," *Mechanism Mach. Theory*, vol. 78, pp. 177–186, Aug. 2014.

[3] W. Ye and Q. Li, "Type synthesis of lower mobility parallel mechanisms: A review," *Chin. J. Mech. Eng.*, vol. 32, no. 1, pp. 1–11, Apr. 2019.

[4] J. M. Hervé, "Analyse structurelle des mécanismes par groupe des déplacements," *Mechanism Mach. Theory*, vol. 13, no. 4, pp. 437–450, Jan. 1978.

[5] J. Hervé, "The lie group of rigid body displacements, a fundamental tool for mechanism design," *Mechanism Mach. Theory*, vol. 34, no. 5, pp. 719–730, Jul. 1999.

[6] J. M. Herve, "Uncoupled actuation of pan-tilt wrists," *IEEE Trans. Robot.*, vol. 22, no. 1, pp. 56–64, Feb. 2006.

[7] C.-C. Lee and J. M. Hervé, "Generators of the product of two schoenflies motion groups," *Eur. J. Mech.-A/Solids*, vol. 29, no. 1, pp. 97–108, Jan. 2010.

[8] C.-C. Lee and J. M. Hervé, "Type synthesis of primitive schoenflies-motion generators," *Mechanism Mach. Theory*, vol. 44, no. 10, pp. 1980–1997, Oct. 2009.

[9] Q. Li, Z. Huang, and J. M. Herve, "Type synthesis of 3R2T 5-DOF parallel mechanisms using the lie group of displacements," *IEEE Trans. Robot. Autom.*, vol. 20, no. 2, pp. 173–180, Apr. 2004.

[10] J. Angeles, "The qualitative synthesis of parallel manipulators," *J. Mech. Des.*, vol. 126, no. 4, pp. 617–624, Aug. 2004.

[11] L. Li, Y. Fang, and L. Wang, "Type synthesis of single-loop 3T1R-parallel mechanisms with a multi-DOF drive system," *Mechanism Mach. Theory*, vol. 163, Sep. 2021, Art. no. 104373.

[12] J. M. Rico, J. J. Cervantes-Sánchez, A. Tadeo-Chavez, G. I. Pérez-Soto, and J. Rocha-Chavarria, "A comprehensive theory of type synthesis of fully parallel platforms," ASME-DETC, Pennsylvania, PA, USA, Tech. Rep., DETC2006-99070, Sep. 2006.

[13] J. M. Rico, J. J. Cervantes-Sánchez, A. Tadeo-Chávez, G. I. Pérez-Soto, and J. Rocha-Chavarría, "New considerations on the theory of type synthesis of fully parallel platforms," *J. Mech. Des.*, vol. 130, no. 11, Sep. 2008, Art. no. 112302.

[14] J. Meng, G. F. Liu, and Z. Li, "A geometric theory for synthesis and analysis of sub-6 DoF parallel manipulators," in *Proc. IEEE Int. Conf. Robot. Autom.*, Barcelona, Spain, Jan. 2006, pp. 2938–2943.

[15] J. Meng, G. Liu, and Z. Li, "A geometric theory for analysis and synthesis of sub-6 DoF parallel manipulators," *IEEE Trans. Robot.*, vol. 23, no. 4, pp. 625–649, Aug. 2007.

[16] Q. Li and J. M. Hervé, "Type synthesis of 3-DOF RPR-equivalent parallel mechanisms," *IEEE Trans. Robot.*, vol. 30, no. 6, pp. 1333–1343, Dec. 2014.

[17] Q. Li and J. M. Hervé, "1T2R parallel mechanisms without parasitic motion," *IEEE Trans. Robot.*, vol. 26, no. 3, pp. 401–410, Jun. 2010.

[18] W. Ye, L. He, and Q. Li, "A new family of symmetrical 2T2R parallel mechanisms without parasitic motion," *J. Mech. Robot.*, vol. 10, no. 1, Feb. 2018, Art. no. 011006.

[19] W. Ye, Q.-C. Li, and X.-X. Chai, "New family of 3-DOF UP-equivalent parallel mechanisms with high rotational capability," *Chin. J. Mech. Eng.*, vol. 31, no. 1, pp. 1–12, Feb. 2018.

[20] Q. Jin and T.-L. Yang, "Theory for topology synthesis of parallel manipulators and its application to three-dimension-translation parallel manipulators," *J. Mech. Des.*, vol. 126, no. 4, pp. 625–639, Jul. 2004.

[21] Q. Jin and T.-L. Yang, "Synthesis and analysis of a group of 3-degree-of-freedom partially decoupled parallel manipulators," *J. Mech. Des.*, vol. 126, no. 2, pp. 301–306, Mar. 2004.

[22] T.-L. Yang, A.-X. Liu, Q. Jin, Y.-F. Luo, H.-P. Shen, and L.-B. Hang, "Position and orientation characteristic equation for topological design of robot mechanisms," *J. Mech. Des.*, vol. 131, no. 2, Feb. 2009, Art. no. 021001.

[23] G. Gogu, "Structural synthesis of fully-isotropic translational parallel robots via theory of linear transformations," *Eur. J. Mech.-A/Solids*, vol. 23, no. 6, pp. 1021–1039, Nov. 2004.

[24] G. Gogu, "Structural synthesis of fully-isotropic parallel robots with Schönflies motions via theory of linear transformations and evolutionary morphology," *Eur. J. Mech.-A/Solids*, vol. 26, no. 2, pp. 242–269, Mar. 2007.

[25] G. Gogu, "Structural synthesis of maximally regular T3R2-type parallel robots via theory of linear transformations and evolutionary morphology," *Robotica*, vol. 27, no. 1, pp. 79–101, Jan. 2009.

[26] F. Gao, J. Yang, and Q. J. Ge, "Type synthesis of parallel mechanisms having the second class GF sets and two dimensional rotations," *J. Mech. Robot.*, vol. 3, no. 1, Feb. 2011, Art. no. 011003.

[27] J. He, F. Gao, X. Meng, and W. Guo, "Type synthesis for 4-DOF parallel press mechanism using GF set theory," *Chin. J. Mech. Eng.*, vol. 28, no. 4, pp. 851–859, Jul. 2015.

[28] J. Yang, F. Gao, Q. J. Ge, X. Zhao, W. Guo, and Z. Jin, "Type synthesis of parallel mechanisms having the first class GF sets and one-dimensional rotation," *Robotica*, vol. 29, no. 6, pp. 895–902, Feb. 2011.

[29] J. Yang, F. Gao, K. Zhu, and B. Liu, "Type synthesis of parallel mechanisms with the first class GF sets and two-dimensional rotations," *Int. J. Adv. Robot. Syst.*, vol. 9, no. 3, p. 61, Jan. 2012.

[30] J. S. Dai, "An historical review of the theoretical development of rigid body displacements from Rodrigues parameters to the finite twist," *Mechanism Mach. Theory*, vol. 41, no. 1, pp. 41–52, Jan. 2006.

[31] S. Yang, T. Sun, and T. Huang, "Type synthesis of parallel mechanisms having 3T1R motion with variable rotational axis," *Mechanism Mach. Theory*, vol. 109, pp. 220–230, Mar. 2017.

[32] S. Yang, T. Sun, T. Huang, Q. Li, and D. Gu, "A finite screw approach to type synthesis of three-DOF translational parallel mechanisms," *Mechanism Mach. Theory*, vol. 104, pp. 405–419, Oct. 2016.

[33] T. Sun and X. Huo, "Type synthesis of 1T2R parallel mechanisms with parasitic motions," *Mechanism Mach. Theory*, vol. 128, pp. 412–428, Oct. 2018.

[34] T. Sun, S. Yang, T. Huang, and J. S. Dai, "A way of relating instantaneous and finite screws based on the screw triangle product," *Mechanism Mach. Theory*, vol. 108, pp. 75–82, Feb. 2017.

[35] T. Sun, S.-F. Yang, T. Huang, and J. S. Dai, "A finite and instantaneous screw based approach for topology design and kinematic analysis of 5-axis parallel kinematic machines," *Chin. J. Mech. Eng.*, vol. 31, no. 1, pp. 1–10, May 2018.

[36] Y. Song, P. Han, and P. Wang, "Type synthesis of 1T2R and 2R1T parallel mechanisms employing conformal geometric algebra," *Mechanism Mach. Theory*, vol. 121, pp. 475–486, Mar. 2018.

[37] Z. Huang and Q. C. Li, "General methodology for type synthesis of symmetrical lower-mobility parallel manipulators and several novel manipulators," *Int. J. Robot. Res.*, vol. 21, no. 2, pp. 131–145, Feb. 2002.

[38] Z. Huang, "Type synthesis principle of minor-mobility parallel manipulators," *Sci. China E*, vol. 45, no. 3, pp. 241–248, 2002.

[39] Z. Huang and Q. C. Li, "Type synthesis of symmetrical lower-mobility parallel mechanisms using the constraint-synthesis method," *Int. J. Robot. Res.*, vol. 22, no. 1, pp. 59–79, Jan. 2003.

[40] Y. Fang and L.-W. Tsai, "Structure synthesis of a class of 4-DoF and 5-DoF parallel manipulators with identical limb structures," *Int. J. Robot. Res.*, vol. 21, no. 9, pp. 799–810, Sep. 2002.

[41] Y. Fang and L.-W. Tsai, "Structure synthesis of a class of 3-DOF rotational parallel manipulators," *IEEE Trans. Robot. Autom.*, vol. 20, no. 1, pp. 117–121, Feb. 2004.

[42] Y. Fang and L.-W. Tsai, "Analytical identification of limb structures for translational parallel manipulators," *J. Robot. Syst.*, vol. 21, no. 5, pp. 209–218, May 2004.

[43] X. Kong and C. M. Gosselin, "Type synthesis of 3T1R 4-DOF parallel manipulators based on screw theory," *IEEE Trans. Robot. Autom.*, vol. 20, no. 2, pp. 181–190, Apr. 2004.

[44] X. Kong and C. M. Gosselin, "Type synthesis of 3-DOF spherical parallel manipulators based on screw theory," *J. Mech. Des.*, vol. 126, no. 1, pp. 101–108, Jan. 2004.

[45] X. Kong and C. M. Gosselin, "Type synthesis of 3-DOF translational parallel manipulators based on screw theory," *J. Mech. Des.*, vol. 126, no. 1, pp. 83–92, Jan. 2004.

[46] X. Kong and C. M. Gosselin, "Type synthesis of 3-DOF PPR-equivalent parallel manipulators based on screw theory and the concept of virtual chain," *J. Mech. Des.*, vol. 127, no. 6, pp. 1113–1121, Nov. 2005.

[47] X. Kong and C. M. Gosselin, "Type synthesis of 4-DOF SP-equivalent parallel manipulators: A virtual chain approach," *Mechanism Mach. Theory*, vol. 41, no. 11, pp. 1306–1319, Nov. 2006.

[48] D. Zeng and Z. Huang, "Type synthesis of the rotational decoupled parallel mechanism based on screw theory," *Sci. China Technol. Sci.*, vol. 54, no. 4, pp. 998–1004, Jan. 2011.

[49] Y. Xu, D. Zhang, J. Yao, and Y. Zhao, "Type synthesis of the 2R1T parallel mechanism with two continuous rotational axes and study on the principle of its motion decoupling," *Mechanism Mach. Theory*, vol. 108, pp. 27–40, Feb. 2017.

[50] F. Xie and X.-J. Liu, "Design and development of a high-speed and high-rotation robot with four identical arms and a single platform," *J. Mech. Robot.*, vol. 7, no. 4, Nov. 2015, Art. no. 041015.

[51] F. Xie, X.-J. Liu, and C. Wang, "Design of a novel 3-DoF parallel kinematic mechanism: Type synthesis and kinematic optimization," *Robotica*, vol. 33, no. 3, pp. 622–637, Mar. 2015.

[52] F. Xie, X.-J. Liu, Z. You, and J. Wang, "Type synthesis of 2T1R-type parallel kinematic mechanisms and the application in manufacturing," *Robot. Comput.-Integr. Manuf.*, vol. 30, no. 1, pp. 1–10, Feb. 2014.

[53] H. Chu, S. Shi, and Y. Zhou, "Digital type synthesis method of twin parallel mechanisms and several novel manipulators," *Mechanism Mach. Theory*, vol. 155, Jan. 2021, Art. no. 104103.

[54] H. Chu, Y. Zhou, and J. Yao, "Type synthesis of metamorphic parallel robots based on the serial-chain database," *Mechanism Mach. Theory*, vol. 181, Mar. 2023, Art. no. 105207.

[55] Z. Huang, Q. Li, and H. Ding, *Theory of Parallel Mechanisms*. Cham, Switzerland: Springer, 2013, pp. 31–36.

[56] F. Aimedee, G. Gogu, J. S. Dai, C. Bouzgarrou, and N. Bouton, "Systematization of morphing in reconfigurable mechanisms," *Mechanism Mach. Theory*, vol. 96, pp. 215–224, Feb. 2016.

[57] H. Chu, B. Qi, X. Qiu, and Y. Zhou, "6-DOF wheeled parallel robot and its automatic type synthesis method," *Mechanism Mach. Theory*, vol. 169, Mar. 2022, Art. no. 104646.

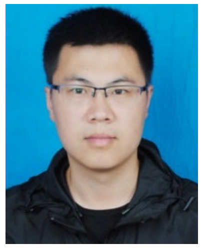

HONGPENG CHU received the B.S., M.S., and Ph.D. degrees in mechanical engineering from Yanshan University, Qinhuangdao, China, in 2014, 2017, and 2022, respectively. He is currently a Postdoctoral Fellow with Tianjin University, Tianjin, China. His research interests include robotics, parallel robots, type synthesis theory, and mechanism design.

YIHUI ZHANG received the B.S. degree in mechanical engineering from the Tianjin University of Technology, Tianjin, China, in 2022. He is currently pursuing the M.S. degree in mechanical engineering with Yanshan University, Qinhuangdao, China. His research interests include robotics and mechanism design.

YULIN ZHOU received the B.S. degree in process and equipment of machinery manufacturing from the Northeast Heavy Machinery Institute, Qiqihar, China, in 1979, and the M.S. and Ph.D. degrees in mechanical engineering from Yanshan University, Qinhuangdao, China, in 1985 and 2008, respectively. He is currently a Professor with Yanshan University. His research interests include bionics and humanoid robots, robotics, heavy equipment design theory, and the application of parallel mechanisms.

DAXING ZENG received the B.S., M.S., and Ph.D. degrees in mechatronic engineering from Yanshan University, Qinhuangdao, China, in 2002, 2004, and 2008, respectively. He is currently a Professor with the School of Mechanical Engineering, Dongguan University of Technology, China. His research interests include the theory of mechanism and machine, parallel mechanism, type synthesis theory, and image processing.